Biosynthesis of Magnetic Nanoparticles for Cancer Detection and Treatment

Thesis

By

John David Obayemi

Department of
Materials Science and Engineering
African University of Science and Technology
Km 10 Airport road
Abuja

In Partial Fulfilment of the Requirement for the Award of Master's Degree in
Materials Science and Engineering

Supervisors:
Professor Wole Soboyejo
Dr Shola Odusanya

Deceember, 2011

DEDICATION

With love,

This research work is specially dedicate to God Almighty who has never fail me and to my quintessence parent Mr David Obayemi and Mrs Deborah Obayemi for their prayers and parental care in helping me realizing my dream. I love u all.

ACKNOWLEDGMENT

All thanks to the omniscience, omnipresence and omnipotent God who is the reason why i am alive today. I remain very grateful to Him for all His good works and favor over my life.

My sincere special gratitude goes to my mentor, father and indefatigable supervisor, Professor Wole Soboyejo who for his patience, understanding, guidance and mentorship lead to the successful completion of this phase of my research. Words cannot truly express my joy and appreciation for knowing and been thought by a genius like you. I strongly believe in all ramifications that the Almighty God will continue to protect, guide, increase and favor you in all your endeavors.

My special thanks goes to my advisor, Dr Shola Odusanya. Where everyone had an advisor, I have a director, friend and uncle who was not only supervising and guiding me, but was always criticizing, encouraging and assisting me during the period of the research.

I also wish to say kudos to my mum and dad, Mr David Obayemi and Mrs Deborah Obayemi through whose union, perseverance, parental care and prayers, i am gradually getting to the promise land. A big thank you goes also to my brothers, Mr Oluwatope David Obayemi, Mr Daniel Obayemi, Mr Solomon Obayemi and to my sisters Mrs Taiwo Adeoye, Mrs Ruth David and Miss Bukola Obayemi.

My earnest appreciation also goes to the entire faculty of Materials Science and Engineering: Professor Kwado Osseo-Asare, Professor Douglas Buttrey, Professor Babatunde Ogunnaike, Professor Thomas Vogt, Dr Zabaze Kana, etc and the students Mr Ampaw Edward, Mr Vodah Emmanuel to mention but a few. You have been wonderful to me throughout my MSc

programme in AUST, God bless you all. My deepest gratitude goes to all my friends especially, Mr Charles and Haruna Yunusa Onuh, Mr Adekunle Opawale, Mr Nanchang Bagudu, Mr Stephen Dawa, Mr Bege Tanko Dogo, Miss Blessing Atoyebi, Miss Jummai Dogo Makama etc, who in one way or the other have inspire me in the course of my studies at AUST.

My profound gratitude also goes to the Director General of SHESTCO Professor Sunday Thomas for giving me and my colleague the opportunity to work in the biotechnology advance laboratory. Also, my thanks go to Dr Nicolas Anuku, Dr Karen Malatesha and their team at Princeton University in the USA and to the entire team at Advance Biotechnology laboratory at SHESTCO specifically, Mr Godwin Etuk-Udo, Mrs Dozie Nwachuckwu, Miss Oluchi, Miss Ngozi, Mr Kama and Miss Amaka Ilogbelu for their immense contribution in making this research a reality.

Finally, I must express my deep appreciation to AUST, STEP B, SHESTCO and the Princeton University in the USA for a wonderful collaboration in making this phase of research a reality.

TABLE OF CONTENTS

LIST OF FIGURES

LIST OF TABLES

ABSTRACT

Chemical and physical methods for the synthesis of magnetic nanoparticles for cancer detection and treatment often involve toxic chemicals, high cost and the formation of non-stable nanoparticles. This prompted the development of fundamental understanding of the synthesis of magnetic nanoparticles, which are biocompatible, cost effective, stable, localized and environmentally friendly in the presence of magnetotactic bacteria.

In this work, fundamental understanding of the underlying mechanisms involved in the formation of magnetic nanoparticles by magnetotactic bacteria are unraveled. Soil dwelling microbes that respond to magnetic pull were cultured in the presence of ferrous salts in a magnetic *spirillum* growth medium (MSGM). A comparative analysis was made whereby a positive control *Magnetospirillum magneticum* and an indigenous isolated strain were used in the biosynthesis of magnetic nanoparticles. The dependence of particle shape and size on pH and time, were elucidated using a combination of transmission electron microscopy (TEM) and UV-visible spectrophotometry. The implications of the results are discussed for the development of magnetic nanoparticles for the detection and treatment of cancer.

CHAPTER ONE

1.0 INTRODUCTION

1.1 Background and Motivation

Nanotechnology has provides solutions to some critical problem in the areas of energy generation [1, 2], information storage [3], environmental remediation [4, 5] and biological application [6] to mention but a few. In the recent years, there has been increasing interest in the development of nanoparticles for potential and emerging applications in medicine [7]. These include potential emerging applications in disease detection and treatment [8, 9], biological labelling [10], biosensors [11] and drug delivery [12].

In the case of magnetic nanoparticles (MNPs), there have been significant efforts to develop magnetic nanoparticles for application in cancer detection via magnetic resonance imaging (MRI) [13] and treatment by hyperthamia [14]. In MRI, the current spatial resolution of detection is of the order of a few millimeters [15]. MNPs have been produced largely from Iron, cobalt, iron oxide (Fe_3O_4) and Fe_3CoO_4 (Yang et al 2006). Their potential has also been explored for use as contrast enhancement agent during MRI of tumour tissue [16] and localized hyperthamia [14] during cancer treatment. Magnetic nanoparticles have been reported to have the ability of binding to drugs, proteins, enzymes, antibodies, or nucleotides and can be directed to an organ, tissue, cells or tumors using an external magnetic field or can be heated in alternating magnetic fields for use in hyperthermia.

Fe_3O_4 MNPs are heat-generating nanoparticles which have the ability to convert electromagnetic energy to heat energy. These MNPs have been found to be efficient in the detection and

treatment of cancer by MRI and simple radiation therapy. In this case of radiation therapy, energy produced is used to destroy the cancer cells and reduce the size of tumours effectively when a cyclic external magnetic field is applied.

In most cases, there are several physicochemical methods that are used for the synthesis of MNPs. These include: microemulsion, sol-gel synthesis, hydrothermal reactions, flow injection synthesis, electrochemical synthesis, pyrolysis, laser pyrolysis, microwave assisted, carbon arc, combustion synthesis, vapour deposition and chemical co-precipitation method [7, 17]. However these synthesis methods often involve the use of toxic chemicals that can have harmful effects on the environment.

There is therefore a need for environmentally friendly methods for the synthesis of magnetic nanoparticles, that has stimulated the recent interest in the biological synthesis of magnetic nanoparticles from magnetotactic bacteria. There is also a need to understand the underlying mechanisms of magnetic nanoparticle formation in the presence of magnetotactic bacteria. To this end, most work in this field has been done in improving the biocompatibility of the materials, but only a few scientific investigations and developments have been carried out to develop a fundamental understanding of the synthesis of magnetic nanoparticles, which are biocompatible, cost effective, stable, localized and environmentally friendly in the presence of magnetotactic bacteria. The need to understand the underlying mechanisms involved in the formation of magnetite nanoparticles by these bacteria will contribute positively in improving the quality of magnetic particles, their size distribution, their shape and surface under certain preexisting conditions. This would lead to characterizing them to get a protocol for the quality control and commercialization of these particles in cancer detection and treatment.

The biomineralization of magnetite has been shown to occur in diverse range of organisms such as algae, insects, mollusks, fish, birds and even humans [18]. However, a considerable amount of

magnetite is deposited by magnetotactic and iron reducing bacteria in nature, (Atul Bharde et al). A survey of the literature showed that iron-reducing bacteria and magnetotactic bacteria responsible for the production of magnetite have been found in various natural environments. These include: freshwater and marine environments, clean and contaminated aquifers, geothermal vents and deep subsurface environments [19, 20]. The Magnetite synthesis in magnetotactic bacteria occurs in a unique intracellular structure called magnetosomes. Magnetosome is a lipid bilayer structure, which houses highly ordered magnetite crystals, aligned parallel to the cellular axis. The magnetite synthesized by magnetotactic bacteria shows species-specific morphology and size variations [20]. In contrast to physiochemical synthesis methods, this biological synthesis of MNPs will be characterized by ambient experimental conditions of temperature, pH and time to observe their effect on nanoparticles morphology.

1.2 Problem Statement and Scope of Work

The objective of this study is to develop a simple and novel approach for the synthesis of magnetic nanoparticles (magnetite) in the presence of magnetotactic bacteria. The study will also develop a fundamental understanding of the effects of pH and reaction time on the shapes and sizes of magnetic nanoparticles produced under well controlled durations of exposure to magnetotactic bacteria. The nucleation and growth of the nanoparticles will be characterized and modelled as well as their potential to target breast cancer and cells.

The organization and scope of this thesis is as follows: First, this chapter presents the background, motivation, problem statement and the scope of the work. Chapter 2 then describes prior work on in the synthesis of magnetic nanoparticles, as well as their magnetic and adhesion

properties. The applications of magnetic nanoparticles are then discussed for the detection and treatment of cancer. This is followed by a description of the experimental procedure in chapter 3. The results and discussion are described in chapter 4 before summarizing the salient conclusions from this work in chapter 5.

1.3 References

[1] Zach,M., Hagglund,C., Chakarov,D. & Kasemo,B. (2006). Nanoscience and nanotechnology for advanced energy systems. Current Opinion in Solid State and Materials Science,10, 132-143.

[2] Serrano,E., Rus,G. & Garcia-Martinez,J. (2009). Nanotechnology for sustainable energy

[3] Sandhu,A. (2008). Data storage: One-track memory. Nature Nanotechnology. doi:10.1038/nnano.2008.120.

[4] D. W. Elliott, W.-X. Zhang, Environ. Sci. Technol. 2001, 35, 4922.

[5] M. Takafuji, S. Ide, H. Ihara, Z. Xu, Chem. Mater. 2004, 16,1977.

[6] Caruthers,S.D., Wickline,S.A. & Lanza,G.M. (2007). Nanotechnological applications in medicine. Current Opinion in Biotechnology,18, 26-30.

[7] Q A Pankhurst1, J Connolly2 et al. Applications of magnetic nanoparticles in biomedicine. Journal of physics d: applied physics. June 2003, J. Phys. D: Appl. Phys. 36-R167–R181.

[8] B. Fadeel, A. E.G. Bennett. Better safe than sorry: Understanding the toxicological properties of inorganic nanoparticles manufactured for biomedical applications. Advanced Drug Delivery Reviews. 2010, 62, 362–374.

[9] Matsunaga, T.,Okamura,Y., Tanaka, T. J. Mater. Chem. **2004**, 14**,** 2099

[10] Qiu H, Rieger B, Gilbert Ret al. PLA-coated gold nanoparticles for the labeling of PLA biocarriers. 2004, Chem Mater 16:850–856

[11] Gomez-Romero P. Hybrid organic-inorganic materials—in search of synergic activity. Adv Mater . 2001, 13:163– 174

[12] Lazaro FJ, Abadia AR, Romero MS, Gutierrez L, Lazaro J, Morales MP Biochim Biophys Acta. 2005, 1740:434–45

[13] T.K. Indira, P.K. Lakshmi. Magnetic Nanoparticles – A Review, International Journal of

Pharmaceutical Sciences and Nanotechnology. 2010, Volume 3 • Issue 3

[14] M. Shinkai, M.Yanase, M. Suzuki, et al. Intracellular hyperthermia for cancer using magnetite cationic liposomes. Journal of Magnetism and Magnetic Materials. 1999, 194, 176184.

[15] D.G. Gadien, NMR and its Applications to Living Systems, Oxford University Press, New York, 2000.

[16] Pardoe H, Clark PR, St Pierre TG, Moroz P, Jones SK Magnetic Resonance Imaging. 2003 21:483–488.

[17] W. Zhou, W. He, S. Zhong, et al. Biosynthesis and magneticproperties of mesoporous Fe_3O_4 composites. Journal of Magnetism and Magnetic Materials. 2009, 321, 1025–1028.

[18] (a) Toress de Araujo, F. F., Pires, M. A., Frankel, R. B., Bicudo, C. E. M. Biophys, J. **1986**, 50, 376. (b) Maher, B., A. Proc. R. Soc. Lond. Biol. **1998**, 265, 733. (c) Lowenstam, H. A., Science **1981**, 211, 1126. (d) Mann, S., Sparks, N. H. C., Walker, M. M., Kirschvinc, J. L. J. Exp. Biol. **1988**, 140, 35. (e) Wiltschko, R., Wiltschko, W. In Magnetic orientation in animals, 1995, Springer, New York. (f) Kirschvinc, J. L., Kobayashi- Kirschvinc, A., Woodford, B., J. Proc. Natl. Acad, Sci. USA **1992**, 89, 7683.

[19] C. Zhang, H. Vali, C. Romanek, T. Phelps and S. Liu, "Formation of signal-domain magnetite by thermophilic bacteriam," American Mineralogist, Vol. 83, pp. 1409-1418, 1998

[20] (a) Blackmore, R. P. Annu. Rev. Microbiol. **1982,** 36, 217.(b) Bazylinski, D. A., Frankel, R. B., Jannasch, H. W. Nature, **1988**, 334, 518. (c) Sakaguchi, T., Burgess, J. G., Matstunaga, T. Nature, **1993**, 365, 47. (d) Schuler, D., Frankel, R. B. Appl. Microbiol. Biotechnol. **1999**, 52, 464. (e) Philse, A. P., Maas, D. Langmuir **2002**, 18, 9977.

CHAPTER TWO

2.0 LITERATURE REVIEW

2.1 Introduction

There has there has been tremendous interest in the synthesis of magnetic nanoparticles for cancer detection and treatment via MRI [1] and hyperthermia [2]. This is due to their unique magnetic properties, that are related to their sizes and shapes distribution. Magnetic nanoparticle (MNPs) exhibit the phenomenon called superparamagnetism. This enable them to remain magnetized even after the application of a magnetic field. This property in a way reduces the risk of the particles not aggregating [Ruiz-Hernandez et al., 2008]. Iron oxide magnetic nanoparticles have been shown to exhibit higher performance in terms of chemical stability and biocompatibility, compared to metallic nanoparticles [Simsek and Kilic, 2005]. This has stimulated an interest in their potential for biomedical applications such as magnetic drug targeting, MRI for clinical diagnosis, hyperthermia anti-cancer strategy and enzyme immobilization [3-10]. Magnetic nanoparticles that are used in bio-applications, are usually made from biocompatible materials such as magnetite for which susceptibility is large (Shaw et al., 2009). This have the capacity of producing high-field magnetic resonance images due to their unique magnetic properties.

2.2 Concept of Electrochemistry

Electrochemistry is a branch of chemistry dealing with chemical reactions that involve electrical current and potentials. In some cases, it is seen as the science that deals with situations where

oxidation and reduction reaction are separated in time and space connected by an external field. The chemical reaction in this sense takes place in solution at an interface of an electron conductor and ionic conductor. During the process of chemical reaction, there is transfer of electrons between the species in solution and the electrode. [11]

2.2.1 Redox Reactions

The term redox simply denotes reduction-oxidation. All chemical reactions or electrochemical processes involve electron transfer to or from a molecule or ion. The resulting change in the oxidation state is due to redox (reduction/oxidation) reactions. This occurs as a result of the application of an external voltage or through the release of chemical energy. During this process, there is a change in oxidation state that takes place in the ions, molecules and atoms. Oxidation and reduction always occur in a paired fashion, such that one species is reduced, while the other is oxidized.

An ion or atom that gives up an electron to another ion or atom has its oxidation state increased, while the recipient of the negatively charged electron has its oxidation state decreased. Thus, the molecules or atoms that lose electrons are known as reducing agents or *reductants,* while the substance that accepts the electrons is called the oxidizing agent or *oxidant*. The oxidizing agent is always being reduced, while the reducing agent is always being oxidized in a reaction. [11]

2.2.2 Basic Medium

In a basic medium, OH^- ions and water are added to half reactions to balance the overall reaction. For example, the reaction between potassium permanganate and sodium sulfite gives;

Unbalanced reaction: $KMnO_4 + Na_2SO_3 + H_2O \rightarrow MnO_2 + Na_2SO_4 + KOH$

Oxidation: $2\ OH^- + SO_3^{2-} \rightarrow SO_4^{2-} + H_2O + 2\ e^-$

Reduction: $3\ e^- + 2\ H_2O + MnO_4^- \rightarrow MnO_2 + 4\ OH^-$

By multiplying electrons to opposite half reactions at the electrode, the combining equation, by the virtue of balancing, gives the overall reaction.

$6\ e^- + 4\ H_2O + 2\ MnO_4^- \rightarrow 2\ MnO_2 + 8\ OH^-$

$6\ OH^- + 3\ SO_3^{2-} \rightarrow 3\ SO_4^{2-} + 3\ H_2O + 6e^-$

The balanced equation becomes

$2\ KMnO_4 + 3\ Na_2SO_3 + H_2O \rightarrow 2\ MnO_2 + 3\ Na_2SO_4 + 2\ KOH$ [11]

2.2.3 Acidic Medium

In an acidic medium, H^+ ions and water are added to half-reactions to balance the overall reaction. For example, when manganese reacts with sodium bismuthate;

Unbalanced reaction: $Mn^{2+}(aq) + NaBiO_3(s) \rightarrow Bi^{3+}(aq) + MnO_4^-(aq)$

Oxidation: $4\ H_2O(l) + Mn^{2+}(aq) \rightarrow MnO_4^-(aq) + 8\ H^+(aq) + 5\ e^-$

Reduction: $2\ e^- + 6\ H^+(aq) + BiO_3^-(s) \rightarrow Bi^{3+}(aq) + 3\ H_2O(l)$

Finally, the reaction is balanced by multiplying the number of electrons from the reduction half reaction to oxidation half reaction and vice versa and adding both half reactions, thus solving the equation.

$8\ H_2O(l) + 2\ Mn^{2+}(aq) \rightarrow 2\ MnO_4^-(aq) + 16\ H^+(aq) + 10\ e^-$

$10\ e^- + 30\ H^+(aq) + 5\ BiO_3^-(s) \rightarrow 5\ Bi^{3+}(aq) + 15\ H_2O(l)$

The balanced reaction is:

$14\ H^+(aq) + 2\ Mn^{2+}(aq) + 5\ NaBiO_3(s) \rightarrow 7\ H_2O(l) + 2\ MnO_4^-(aq) + 5\ Bi^{3+}(aq) + 5\ Na^+(aq)$ [11]

2.2.4 Neutral Medium

A typical example of neutral medium is the complete combustion of propane

Unbalanced reaction: $C_3H_8 + O_2 \rightarrow CO_2 + H_2O$

Reduction: $4\ H^+ + O_2 + 4\ e^- \rightarrow 2\ H_2O$

Oxidation: $6\ H_2O + C_3H_8 \rightarrow 3\ CO_2 + 20\ e^- + 20\ H^+$

Here, electrons which were used to compensate oxidation changes are multiplied to opposite half reactions, thus solving the equation.

$20\ H^+ + 5\ O_2 + 20\ e^- \rightarrow 10\ H_2O$

$6\ H_2O + C_3H_8 \rightarrow 3\ CO_2 + 20\ e^- + 20\ H^+$

The balanced equation is;

$C_3H_8 + 5\ O_2 \rightarrow 3\ CO_2 + 4\ H_2O$ [11]

2.3 Synthesis of Magnetic Nanoparticles

Several methods are used for the synthesis of magnetic nanoparticles. They include physical, chemical, biological and hybrid methods [90 – 93]. Physical methods of synthesis deals with generation of magnetic nanoparticles in the gas or solid phase using high-energy treatments such as Condensation methods, Methods of nanodispersion of a compact material etc. In contrast, the chemical synthesis of nanoparticles involves reaction that are carried out in solutions at moderate

temperature. Biological methods of synthesis involve of the use plants and microorganisms in the synthesis of magnetic nanoparticles, While hybrid methods involve some combinations of any of the above methods. A review of some the physical, chemical methods of synthesis followed by biological synthesis are presented in this work.

2.3.1 Physical and Chemical Methods of Synthesis

Some popular physical and chemical methods of synthesis of magnetic nanoparticles are highlighted in this research. These include: microemulsion method, sol-gel method, co-precipitation methods, thermal decomposition and Solvotherma methods [].

2.3.1.1 Microemulsion Method

The microemulsion methods, involes the use of thermodynamically stable isotropic liquid mixture of water or aqueous phases, (oil with surfactant and cosurfactant) in the formation of nanoparticles. In this method, surfactants tend to form reverse micelles, while the cosurfactants reduce the electrostactic repulsion force between the surfactants molecules. Particles size and morphology can be controlled under certain conditions using this method.

The microemulsion method can be direct, reverse or bicontinous, depending on what solution is dispersed in the other. The most frequently used method for the synthesis of magnetic nanoparticles is the reverse microemulsion. In this method, water is dispersed in oil (w/o). The method is also referred as reverse micelle solution. The production of magnetic and nanosized particles through this route has been proved to be adequate, versatile and simple [12-17]. Tartej et alave halso observed that, this is achievable when fine droplets at the micro level of the

aqueous phase, are trapped within the area in which surfactant molecules are dispersed in a continuous oil phase. They showed that the surfactant-stabilized microcavities tend to enhance a confinement effect that limits particle nucleation, growth and agglomeration. This was demonstrated by using a micellar solution (a ferrous sulfate, $Fe(DS)_2$), preparing a nanosized magnetic particles whose sizes were controlled partially by the surfactant concentration and temperature [18]. Higgins in 1997 also noted that, microemulsions are produced spontaneously without the need for significant mechanical agitation. The microemulsions method is therefore easy to scale up for large scale production using relatively inexpensive and simple equipment.

2.3.1.2 Sol-gel Method

The Sol-gel method is a wet-chemical technique popularly used in the field of materials science and engineering. Usually applicable in most technology like ceramics technology, reactive material and separation, chromatography, nanotechnology etc [19], it is often use in the synthesis of magnetic nanoparticles (metal oxide), heteroelement and some fused bimetallic particles [20]. Conventionally, sol-gel processing refers to the hydrolysis and condensation of metal alkoxide. The synthesis of magnetic nanoparticles starts from a colloidal reaction which serve as the precursor for an integrated network of either discrete particles or network polymers [21]. Klein et al revealed in 1994 that the sol-gel method is a cheap and low temperature technique that controls the products chemical composition. It can be used for the synthesis of nanoparticles for applications in biosensors, medicine, electronics, optics, electronics, and photovoltaic [22].

2.3.1.3 Co-precipitation Method

This co-oprecipitation method is one of the most widely used in the synthesis of magnetic nanoparticles. This is a water- based method, where metal oxide precipitation and a polymerization reaction are carried out at the same time, so that the developing particles are trapped inside the tiny polymer beads. The synthesis in this case, is divided into two parts. Firstly, ferrous metal hydroxide suspensions are partially oxidized accordingly with different oxidizing agents [23]. Secondly, stoichiometric mixtures of ferric and ferrous hydroxide are aged in aqueous media, yielding spherical magnetite particles with homogenous sizes [24]. The chemical equation for the latter is given by [25]

$2Fe^{3+} + Fe^{2+} + 8OH^{-} = Fe_3O_4 + 4H_20$

The sizes and shapes of the nanoparticles can be controlled by changing the pH, ionic strength, temperature and other pre-existing conditions [26]. However, the crystallinity and size uniformity of the magnetic nanoparticles are poor, and there seems to be the problem of aggregation produced by these methods [26].

2.3.1.4 Thermal Decomposition

This method could also be referred to as thermolysis. This often involves by an a chemical decomposition which is endothermic reaction that is caused by heat. The heat is used to break down the chemical bond in the compound. However, in cases in which the decomposition reaction are is exothermic, a positive feedback loop that is created, that can lead to a thermal runaway and an explosion, in some cases. The decomposition of iron precursors to obtain

magnetic nanoparticles in the presence of hot organic surfactants, results in samples with good size control, narrow size distribution (5-12 nm) and good crystallinity. The nanoparticles are also easily dispersed. The resulting product here has a good potential applications in nanomedicine e.g in cell separation and magnetic resonance imaging [27]. Sun et al [28] worked earlier on thermal decomposition. Hence the resulting method is often refered to as the Sun method. Their method [28] involves the high temperature (> 220^{o}C) decomposition of an organic iron precursor in the presence of oleic acid that decomposes to form organic ligands [28]. In this case, the nanoparticles produced avoid aggregation when the hydrophobic ligands form a dense coating around. However, the nanoparticles that are synthesized are soluble only in nonpolar solvents due to the coatings involved. To solve this problem, hydrophilic polymer coatings have been proposed [29].

There are two popular adopted approaches in the production of magnetic nanoparticles by thermal decomposition [29]. Firstly, by the thermal decomposition of metal carbonyl precursors, followed by an oxidation step in air [29], or oxidation by an oxidant at elevated temperatures [30]. The second is decomposition of precursors with a cationic metal center in the absence of reducing agents [31]. Another special case of thermolysis is called pyrolysis. It involves the simultaneous change of chemical composition and physical phase, and is a irreversible process. It involves thermochemical decomposition of organic materials at elevated temperatures, without the participation of oxygen.

2.3.1.5 Solvothermal Synthesis

This method is also known as hydrothermal process. It involves he synthesis of nanoparticles from chemical reactions that occur under high temperature and pressure. The temperature is

typically above the boiling point of the solvent. Also, due to the high pressure involved, the reaction are carried out in an autoclave. Wang et al, established this process as one of the reliable ways to grow crystals of many materials, one of which is magnetic nanoparticles. The resulting crystalline materials are dislocation free single crystal particles and grains that have a higher levels of crystallinity than particles produced from other methods [32-38]. However, the reaction typically occurs at a slow rate over a narrow regime of temperatures [33].

2.3.2 Biological Synthesis

Until recently, chemical and physical methods were the popular methods of synthesizing magnetic nanoparticles. However, they often involved the use of toxic chemicals. Furtheremore, the cost, localization and the stability of MNPs produced by the physical and chemical methods, tend to limit their potential greatly for biomedical applications like drug delivery system or magnetic resonance imaging (MRI). Also, physical and chemical methods typically require harsh experimental conditions of high temperature and pressure and therefore are considered to be energy intensive and expensive. Furthermore, most chemical synthesis procedures employ specialty chemicals and often yield particles in non-polar organic solutions [21]. These tends to preclude and limit their application in biomedicine. Finally, many of the surfactants that are used to control size and shape are toxic.

In contrast, the biosynthesis of nanoparticles from magnetotactic bacteria produces superparagmatic magnetite nanoparticles with controlled sizes and shapes under non toxic conclusions. These nanoparticles formation pathway are non-toxic and low cost. They can also be used to form magnetic nanoparticles wiyh range of sizes. The particles generated by these

processes have higher catalytic reactivity, greater specific surface area and an improved contact between the enzyme and metal salt in question, due to the bacterial carrier matrix [39, 40].

Biosynthesis of magnetic nanoparticles can be carried out using plants or micro-organisms. The nanoparticles can also form intracellularly or extracellularly on micro-organisms. Since the micro-organisms grab target ions from their environment or medium, they can process metal ions into the elemental metals through enzymes that are generated by cell activities. The nanoparticles are form intracellularly, when the process involve the transportation of ions into the microbial cell to form nanoparticles in the presence of enzymes. In contrast, the nanoparticles can also form extracellularly when they involve the trapping of metal ions on the surfaces of cells and the reduction of ions in the presence of enzymes [40-42].

Table 2.1 below highlights different micro-organisms that have been used to synthesize magnetite nanoparticles. The resulting shapes and sizes (produced extracellularly or intracellularly) are also summarized in table 2.1.

Table 2.1: List of microorganisms that have been used to synthesize magnetite nanoparticles

Microorganism	**Product**	**Culturing tempt(°C)**	**Size range(nm)**	**Shape(s)**	**Location**	**References**
Shewanella oneidensis	Fe_3O_4	28	40-50	rectangular, rhombic, hexagonal	Extracellular	[43]
QH-2	Fe_3O_4	22-26	81± 23×58±20	rectangular	Intracellular	[44]
Recombinant AMB-1	Fe_3O_4	28	20	cubo-octahedral	Intracellular	[45]
yeast cells	Fe_3O_4	36	Not Available	wormhole-like	Extracellular	[46]
WM-1	Fe_3O_4	28	54 ± 12.3× 43 ± 10.9	cuboidal	Intracellular	[47]
HSMV-1	Fe_3O_4	63	113±34 ×40 ± 5	Bullet-shaped	Intracellular	[48]

Reports have shown that, apart from magnetotactic bacteria that synthesize magnetic nanoparticles, an aerobic and acid tolerant bacteria, *Leptothrix ochracea* [49] and *Leptospirillum ferriphilum* [50], can also produce magnetic nanoparticles. Another aerobic bacterium called *Antinobacter* species was found by Bharde et al [51, 52] to synthesize magnetite and gregite, which has protein coatings.

They also reported that few fungi, *Fusarium oxysporum* and *Verticillium species* when

challenged with mixture of potassium ferricyanide/ferrocyanide at room temperature produce magnetite nanoparticles extracellularly. Bharde et al [51, 52] also explored the possibility of using mixture of ferric and ferrous chloride in the synthesis of magnetite. However the particles formed were irregular in shape and had irregular crystal structures [53].

2.3.2.1 Magnetotactic Bacteria (MTB) and Magnetite Particles

Magnetotactic bacteria were discovered by R. P. Blackmore in 1975 [54]. They are gram negative, microaerophilic, motile and exhibit aquatic life form that swims along geomagnetic field lines of the earth. They are cosmopolitan in distribution and are found in aquatic environments containing water with pH close to neutral value and water that is well oxygenated or not strongly polluted with chemicals or contaminants [55]. They are magnetotaxis in nature, meaning they respond to magnetic pull in the presence of field. They also produce an intracellular structure, which houses magnetic nanoparticles, called magnetosomes. Magnetotactic bacteria are a heterogeneous group of fastidious prokaryotes that display a myriad of cellular morphologies, including coccoid, rod shaped, vibriod, helical and even multicellular [56].

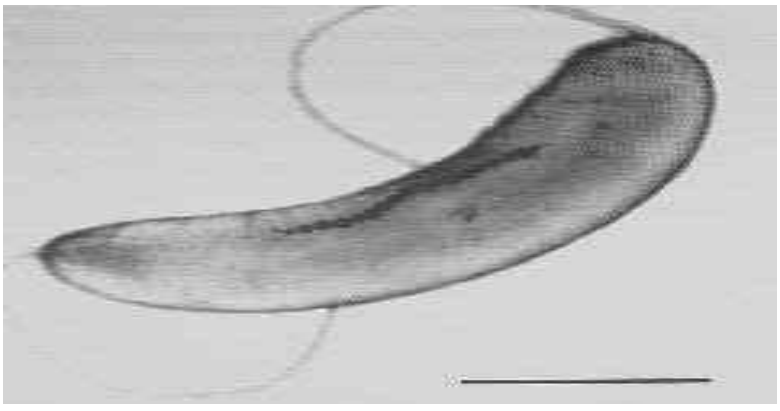

Figure 2.1: A typical magnetotactic bacteria (Picture by Richard B. Frankel department of physics, Cal Poly State University, San Luis Obispo CA. Adapted from [73])

In most of the magnetotactic bacteria, the magnetosomes are arranged in single or multiple chains. Magnetic interactions between the magnetosomes, in chains cause their magnetic dipole moments to orient parallel to each other along the length of the chain. Thus, the overall magnetic moment is maximized by linear arrangements of magnetosomes, enabling cells as tiny, self-propelled magnetic compass needles [57]. Magnetite crystals synthesized inside the magnetosomes exhibit unusual crystal morphologies [58]. These were initially defined as intracellular, magnetic single-domain crystals of a magnetic iron mineral (magnetite) that are enveloped by a trilaminate structures in the magnetosome membrane [57].

2.3.2.2 Magnetospirillum Magneticum

This is a typical species of magnetotactic bacteria [72]. *Magnetospirillum magneticum* are microaphilic and motile in nature. They are strain AMB-1, which are Gram negative and survive in a chemically stratified water column [73]. Research has shown that they grow effectively in the anaerobic lower regions, and aerobically in the upper bodies of some water. They are major agents in the global iron cycle [72], converting the iron in the environment to magnetite or gregite within the magnetosomes. They are also said to be magnetotaxis; a phenomenon that makes them to respond to magnetic pull [72]

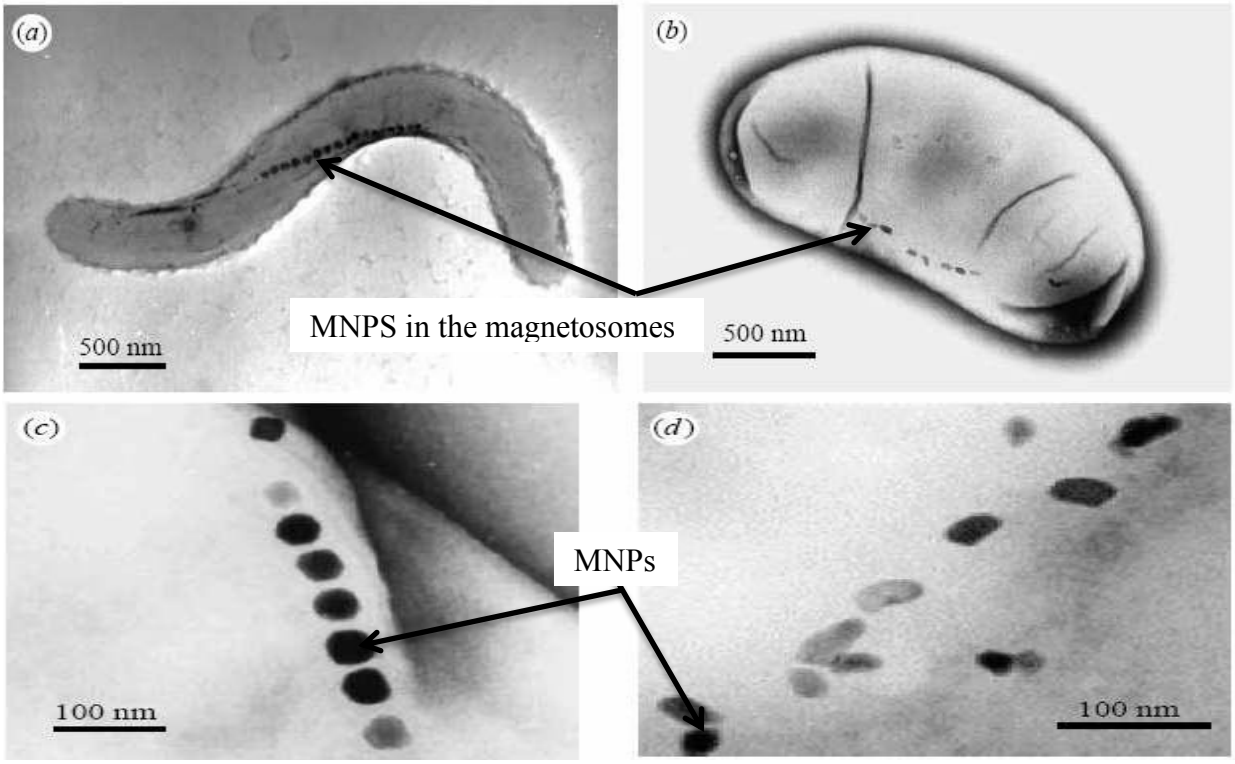

Figure 2.2: TEM images of magnetotactic bacteria. (a) Magnetospirillum magneticum strain AMB-1 and (b) Desulfovibrio magneticus strain RS-1. BacMPs of (c) the AMB-1 strain and (d) the RS-1 strain. Adapted from [74]

2.4 Magnetic Nanoparticles for Cancer Detection and Treatment

Magnetic nanoparticles (MNPs) depending of their synthesis pathway are explored for potential applications as contrast agents and drug delivery agents in localized cancer therapy as good contrast agents prior to their use as drug delivery agents for localized therapy [59, 60]. In the case of potential applications as contrast agents in magnetic resonance imaging.[75, 76], Meng et al. [77] have shown that superparamagnetic iron oxide contrast agents can provide sub-millimeter resolution in the imaging of breast cancer tissue in mice. Other researchers have shown that magnetic nanoparticles can be combined and conjugated together to cancer drugs and [60].

2.4.1 Magnetic Resonance Imaging (MRI)

Magnetic Resonance Imaging (MRI) in a more general sense is a technique that utilizes pulses of radio wave energy and magnetic fields to diagnose disease by creating images of structures and organs inside the body. It is also a non-destructive and non-invasive approach that reconstructs three-dimensional and two-dimensional pictures of internal living structures without restriction in depth or volume. It has been described as a process by which images are generated, based on the nuclear magnetic resonance signals of the water proton (1H) nuclei in the specimen [61].

MRI, in some cases, gives some details that are not possible with other imaging methods like ultrasound, x-ray or computed tomography (CT) scans. When diagnosing with MRI, the part of the body involved is subjected to strong magnetic field. MRI is essentially used to probe tumors, bleeding, injury, infection or blood vessel diseases [78 – 81]. Research has shown that, to enhance the images during MRI, a contrast material or agent is needed. This is why, in a standard clinical MRI scan, contrast media commonly used. The most commonly used contrast agent are gadolinium (Gd) chelates. Due to the problem of agglomeration or accumulation in the liver, incorporated with their non-specificity, they provide a short time imaging window [62, 63]. For these reasons, magnetic nanoparticles (Fe_3O_4) are used *in-vivo* as contrast agents to produce local changes of the proton resonance in MRI for disease diagnosis. This makes MRI the most successful imaging method currently in use. Superparamagnetic iron oxides have been reported to be effective in MRI agents [78]. Meng et al fully described *in vivo* and *in vitro* studies of the intake of LHRH–SPIONs and SPIONs into breast cancer cells. From their findings, they show how MNPs enter and accumulate in the breast cancer cells as a function of particle size and exposure time. They also explained that the uptake of the LHRH–SPIONs is also shown to be

much greater than that of the unconjugated SPIONs in both *in vitro* and *in vivo* cases. The increased uptake of intracellular accumulated LHRH–SPIONs is shown to provide T2 contrast enhancement that could lead to improved spatial resolution in MRI by classical T2 imaging. Such improved detection could be very significant for the early detection of cancer [77]. Soboyejo et al [94] in another approach see the effectiveness of MRI in breast cancers diagnosis and treatment with hormone-conjugated nanomaterials. They stated that LHRH-SPIONs effectively has the potential to target cancer cells in both the primary breast tumors and the lung metastases using TEM to measure sub-cellular distributions of SPIONs in the tumors and tissues. In a similar breast cancer study, Zhou et al revealed that accumulation of individual LHRH-magnetic nanoparticles in the nucleus of liver cells suggests that LHRH-MNPs are also potential carriers for effectively delivering drugs or DNA to liver cells with diseases [95].

2.4.2 Hyperthermia

The term hyperthermia simply referred to as treatment by heat in cancer therapy [82]. It involves the exposure of cancer cells/tissue to temperatures of about 41 – 46 ^{o}C so as to kill or shrunk them [64, 83]. Hyperthermia can be used to treat cancer by local or regional means. These are called local and regional hyperthermia. Local hyperthermia also known as thermal ablation is used to destroy tumors in a specific area. While, regional hyperthermia occurs when the regional body temperature is raised beyond the normal body temperature, so as destroy cancer cells/tissue.

Conventional hyperthermia, incorporated with magnetic nanoparticles (superparamagnetic nanoparticles) truly offers immense advantages in specific localized cancer treatment.

Rosensweig [85], superparamagnetic iron oxides nanoparticles show impressive levels of heating at low magnetic fields as compared to ferromagnetic material which require much higher magnetic field strength for effective heat generation. The amount of current resulting to heat generation is proportional to the size of the magnetic field and the size of the object [84]. Man Von Ardenne [66] in the eighteen century was the pioneer to specifically treat cancer patients by this method. This was followed chemotherapeutics approach in the treatment of cancer. The chemotherapeutic technique is known to have damage normal organs and tissue by causing necrosis, coagulation and carbonization to the normal tissue of the patient during the therapy. The reason is because the therapeutic temperature is 54 ^{o}C and the treatment is not localized [65]. However, studies have shown that the optimal temperature range for hyperthermia is between 43 – 44 ^{o}C [64] within this temperature regime, the programmed cell death that occurs, has been shown to be effective in cancer treatment [83]. More recently, Jordan et al [66] in 1999 revealed that magnetic nanoparticles can be used to target cancer cells via immobile specific targeting functional groups. This is due to their higher specific adsorption rates when compared to those of bulk particles.

2.4.3 Drug Delivery

There is need to deliver the drugs precisely and safely to their target site at the right time and controlled release so as to achieve the maximum therapeutic effect. Even though Paul Ehrlich [67] was the first to be recognized for development of magnetic drug delivery systems, Freeman et al [67] in 1960 also proposed that magnetic particles (Fe_3O_4) could be used for localized treatment, with the aid of magnetic field.

Extensively, localized cancer drug delivery systems offers numerous advantages over bulk chemotherapy. This include the reduction of short and long term effects, and a reduction in the amount of drug that is needed to have a therapeutic effect. These possibilities have stimulated extensive interest in the development of nanoparticles for localized cancer treatment. Some of the drug delivery systems available at the moment include liposomes systems, drug conjugates, controlled delivery of cancer therapeutics and transdermal drug delivery patches using controlled released microchips [68]. One of the main limitations of magnetic drug delivery, is the strength of the external field that can be applied to obtain the necessary magnetic gradients that are needed to control the residence times of the nanoparticles in the desired area or which triggers the drug desorption. Neuberger et al suggested that this can be overcome partly by the use of hybrid nanoparticles with permanent Nd-Fe-B shell that encapsulate superparamagnetic iron oxide nanoparticles core [69].

2.5 Magnetic Nanoparticles and Properties

Magnetic nanoparticles (MNPs) are engineered particulate materials with sizes 1 nm to 100 nm. Their magnetic properties can be manipulated to perform special functions (biomedical and non-biomedical applications) in the presence of external magnetic fields. This is because of their their unique magnetic properties.

Magnetite, a good example of MNPs is known to have an inverse spinel ferrite structure with oxygen forming a face center cubic system. The tetrahedral sites are all occupied by Fe^{3+} while Fe^{3+} and Fe^{2+} occupy the entire octahedral site (Banerjee and Moskowitz, 1985). MNPs, which are small, on the order of tens of nanometers, are ferrimagnetic or ferromagnetic in nature with a single magnetic domain and ability to maintain one large magnetic moment. In a ferromagnetic material, all the atomic moments are aligned without an external magnetic fields while a

ferrimagnetic material is similar to ferromagnetic one, but has two different types of atoms with opposing magnetic moments. If the magnetic moment has the same magnitude and the net magnetic moment is zero, the crystal is called antiferromagtic material [70].

The magnetic properties of nanoparticles are classified based on their magnetic susceptibility (X), which is express as the ratio of the magnetization (M) to the applied magnetic field (H). In ferrimagnetic and ferromagnetic materials, the magnetic moments align parallel to H, coupling interactions magnetic state. The X of materials depends on their temperature, H and atomic structures.

A typical example of MNPs used for cancer detection and treatment is called superparamagnetic iron oxides nanoparticles (SPIONs). SPIONs are non-magnetic particles, which can be readily magnetized in the presence of an external magnetic field. They are of the order of 1 to about 30 nm, and are the most promising agents in the detection and treatment of cancer. The size reductions in magnetic materials result in the formation of SPIONs which are single domain particles and have no hysteresis loop [70]. This phenomenon occurs when applied field or thermal fluctuations can easily move the magnetic moments of the nanoparticles away from the easy axis [71]

2.6 Concept of Nucleation and Growth in Nanoparticles

Nucleation and growth characterize the stages of phase transformation that describe the formation of new phases. The initial stage of nucleation involves the formation of critical embroyo sizes, prior to the growth phase.

There are generally two types of nucleation processes. They are homogenous and heterogeneous

nucleation. Homogenous nucleation evolves from fluctuations of molecules and atoms, while heterogeneous nucleation arises as a result of nucleation sites (small particles). Homogenous nucleation is difficult, but heterogeneous nucleation is easier and common. This is because more energy is required to create new surfaces during homogeneous nucleation [86, 87].

Homogeneous nucleation is applicable in some chemical synthesis of magnetic nanoparticles. It occurs due to the driving force of the thermodynamics ΔG (free energy change) given as the condition of free energy due to the new surface and the new volume formed. However, in some cases, heterogeneous nucleation is applicable to the formation of magnetic nanoparticles [88, 89].

2.7 References

[1] Gleich B, Weizenecker J (2005) Nature 435:1214–1217

[2] Pardoe H, Clark PR, St Pierre TG, Moroz P, Jones SK (2003) Magn Reson Imaging 21:483–488

[3] D. K. Kim, Y. Zhang, J. Kehr, T. Klason, B. Bjelke, M. Muhammed, J. Magn. Magn. Mater.225 (2001) 256.

[4] C. H. Reynolds, N. Annan, K. Beshah, J. H. Huber, S. H. Shaber, R. E. Lenkinski, J. A. Wortman, J. Am. Chem. Soc. **122** (2000) 8940.

[5] A. S. Lubbe, C. Bergemann, H. Riess, F. Schriever, P. Reichardt, K. Possinger, M. Matthias, B. Dorken, F. Herrmann, R. Gurtler, P. Hohenberger, N. Haas, R. Sohr, B. Sander, A. J. Lemke, D. Ohlendorf, W. Huhnt, D. Huhn, Cancer Res. **56** (1996) 4686.

[6] C. Bergemann, D. Muller-Schulte, J. Oster, L. Brassard, A. S. Lubbe, J. Magn. Magn. Mater, 194 (1999) 45.

[7] D. C. F. Chan, D. B. Kirpotin, P. A. Bunn, J. Magn. Magn. Mater. 122 (1993) 374.

[8] A. Jordan, R. Scholz, P. Wust, H. Schirra, T. Schiestel, H. Schmidt, R. Felix, J. Magn. Magn. Mater. 194 (1999) 185.

[9] A. Dyal, K. Loos, M. Noto, S. W. Chang, C. Spagnoli, K. V. P. M. Shafi, A. Ulman, M. Cowman, R. A. Gross, J. Am. Chem. Soc. 125 (2003) 1684.

[10] M. Wakamatsu, N. Takeuchi, S. Ishida, Rep. Asahi Glass Found. 56 (1990) 243.

[11] http://en.wikipedia.org/wiki/Electrochemistry

[12] Lisiecki I and Pileni M P 1993 J. Am. Chem. Soc. 7 115

[13] Zhang K, Chew C H, Xu G Q, Wang J and Gan L M 1999 Langmuir 15 3056

[14] Zarur A J and Ying J Y 2000 Nature 403 65

[15] Tartaj P and De Jonghe L C 2000 J. Mater. Chem. 10 2786

[16] Tartaj P and Tartaj J 2002 Chem. Mater. 14 536

[17] Pileni M P 2003 Nature Mater. 2 145

[18] Pileni M P 1993 *J. Phys. Chem.* 97 6961

[19] D R Uhlmann, G Teowee, J Boulton J. Sol-Gel Sci. Technol. 8 1083 (1997)

[20] Bose, S Bid, S K Pradhan,M Pal, D Chakravorty J. Alloys Compd. 343 192 (2002)

[21] Brinker, C.J.; Scherer, G. W. Sol-Gel Science: The Physics and Chemistry of Sol-Gel Processing. Academic Press, 1990, ISBN 0121349705.

[22] Klein, L. Sol-Gel Optics: Processing and Applications. Springer Verlag. 1994, ISBN 0792394240

[23] Sugimoto, T (1980). "Formation of uniform spherical magnetite particles by crystallization from ferrous hydroxide gels*1". Journal of Colloid and Interface Science 74: 227. doi:10.1016/0021-9797(80)90187-3.

[24] Massart, R.; Cabuil, V.J.Chem.Phy.1987, 84,967

[25] Laurent, Sophie; Forge, Delphine; Port, Marc; Roch, Alain; Robic, Caroline; Vander Elst, Luce; Muller, Robert N. (2008). "Magnetic Iron Oxide Nanoparticles: Synthesis, Stabilization, Vectorization, Physicochemical Characterizations, and Biological Applications". Chemical Reviews **108** (6): 2064–110. doi:10.1021/cr068445e. PMID 18543879

[26] Jolivet J P 2000 Metal Oxide Chemistry and Synthesis: From Solutions to Solid State (New York: Wiley)

[27] Laurent, Sophie; Forge, Delphine; Port, Marc; Roch, Alain; Robic, Caroline; Vander Elst, Luce; Muller, Robert N. (2008). "Magnetic Iron Oxide Nanoparticles: Synthesis, Stabilization, Vectorization, Physicochemical Characterizations, and Biological Applications". Chemical

Reviews **108** (6): 2064–110. doi:10.1021/cr068445e

[28] S. Sun at el -Nanoparticles," Journal of the American Chemical Society, 126, pp. 273–279, 2004

[29] F. Davar, Z. Fereshteh, M. Salavati-Niasari, J. Alloys Compd. 476 (2009) 797.

[30] T. Hyeon, S.S. Lee, J. Park, Y. Chung, H.B. Na, J. Am. Chem. Soc. 123 (2001) 12798.

[31] S. Sun, H. Zeng, D.B. Robinson, S. Raoux, P.M. Rice, S.X. Wang, G. Li, J. Am. Chem. Soc. 126 (2004) 273.

[32] K. Butter, K. Kassapidou, G.J. Vroege, A.P. Philipse, J. Colloid Interface Sci. 287 (2005) 485.

[33] B. Mao, Z. Kang, E. Wang, S. Lian, L. Gao, C. Tian, C. Wang, Mater. Res. Bull. 41 (2006) 2226.

[34] H. Zhu, D. Yang, L. Zhu, Surf. Coat. Technol. 201 (2007) 5870.

[35] S. Giri, S. Samanta, S. Maji, S. Ganguli, A. Bhaumik, J. Magn. Magn. Mater. 285 (2005) 296.

[36] J. Wang, J. Sun, Q. Sun, Q. Chen, Mater. Res. Bull. 38 32 (2003) 1113.

[37] F. Gözüak, Y. Köseoğlu, A. Baykal, H. Kavas, J. Magn. Magn. Mater. 321 (2009) 2170.

[38] J. Wang, F. Ren, R. Yi, A. Yan, G. Qiu, X. Liu, J. Alloys Compd. 479 (2009) 791

[39] R. Bhattacharya, P. Mukherjee. Biological properties of ―naked‖ metal nanoparticles. Advanced Drug Delivery Reviews. 2008, 60, 1289–1306.

[40] K. Simkiss, K.M. Wilbur. Biomineralization. Academic, New York, 1989.

[41] S. Mann. Biomineralization: Principles and Concepts in Bioinorganic Materials Chemistry, Oxford Univ. Press, Oxford, 2001.

[42] X. Zhang, S. Yan, R. D. Tyagi, et al. Synthesis of nanoparticles by microorganisms and their

application in enhancing microbiological reaction rates. Chemosphere. 2011, 82, 489–494.

[43] T. P. Gonzalez, C. J.Lopez, A. L. Neal, et al. Magnetite biomineralization induced by Shewanella oneidensis. Geochimica et Cosmochimica Acta. 2010, 74, 967–979.

[44] K. Zhu, H. Pan, J. Li, et al. Isolation and characterization of a marine magnetotactic spirillum axenic culture QH-2 from an intertidal zone of the China Sea. Research in Microbiology. 2010, 161, 276-283.

[45] Y. Amemiyaa, A. Arakakia, S. Sarah et al. Controlled formation of magnetite crystal by partial oxidation of ferrous hydroxide in the presence of recombinant magnetotactic bacterial protein Mms6. Biomaterials. 2007, 28, 5381–5389.

[46] W. Zhou, W. He, S. Zhong, et al. Biosynthesis and magneticproperties of mesoporous Fe_3O_4 composites. Journal of Magnetism and Magnetic Materials. 2009, 321, 1025–1028.

[47] W. Li, L. Yu, P. Zhou, et al. A Magnetospirillum strain WM-1 from a freshwater sediment with intracellular magnetosomes. World Journal Microbiol Biotechnol. 2007, 23, 1489–1492.

[48] C.T. Lefèvre, F. Abreu, M.L. Schmidt, et al. Moderately Thermophilic Magnetotactic Bacteria from Hot Springs in Nevada. Applied and Environment Microbilogy. 2010, 76, 3740–3743.

[49] Hashimoto,H., Yokoyama,S., Asaoka,H., Kusano,Y., Ikeda,Y., Seno,M., Takada,J., Fujii,T., Nakanishi,M. & Murakami,R. (2007). Characteristics of hollow microtubes consisting of amorphous iron oxide nanoparticles produced by iron oxidizing bacteria, Leptothrix ochracea. Journal of Magnetism and Magnetic Materials,310, 2405-2407.

[50] Gao,J., Xie,J.P., Ding,J.N., Kang,J., Cheng,H.N. & Qiu,G.Z. (2006). Extraction and purification of magnetic nanoparticles from strain of Leptospirillum ferriphilum. Transactions of Nonferrous Metals Society of China,16, 1417-1420.

[51] Bharde,A., Wani,A., Shouche,Y., Joy,P.A., Prasad,B.L. & Sastry,M. (2005). Bacterial aerobic synthesis of nanocrystalline magnetite. Journal of the American Chemical Society,127, 9326-9327.

[52] Bharde,A., Parikh,R.Y., Baidakova,M., Jouen,S., Hannoyer,B., Enoki,T., Prasad,B.L., Shouche,Y.S., Ogale,S. & Sastry,M. (2008). Bacteria-mediated precursor-dependent biosynthesis of superparamagnetic iron oxide and iron sulfide nanoparticles. Langmuir,24, 5787-5794.

[53] Bharde,A., Rautaray,D., Bansal,V., Ahmad,A., Sarkar,I., Yusuf,S.M., Sanyal,M. & Sastry,M. (2006). Extracellular biosynthesis of magnetite using fungi. Small,2, 135-141.

[54] Blackmore, R. P. Science, 1975, 190, 377.

[55] Blackmore, R. P. Science, 1975, 190, 377.

[56] (a) Bazylinski, D. A., Garratt-Reed, A., Frankel, R. B. Microscopy Res. Tech. 1994, 27, 389. (b) Spring, S., Schleifer, K. H. Appl. Microbiol. 1995, 18, 147

[57] (a) Moskowitz, B. M. Rev. Geophy, 1995, 33, 123. (b) Bazylinski, D. A., Frankel,

[58] (a) Blackmore, R. P. Annu. Rev. Microbiol. 1982, 36, 217.(b) Bazylinski, D. A., Frankel, R. B., Jannasch, H. W. Nature, 1988, 334, 518. (c) Sakaguchi, T., Burgess, J. G., Matstunaga, T. Nature, 1993, 365, 47. (d) Schuler, D., Frankel, R. B. Appl. Microbiol. Biotechnol. 1999, 52, 464. (e) Philse, A. P., Maas, D. Langmuir 2002, 18, 9977.

[59] Meyers, P. H., et al., Am. J. Roentgenol. Radium Ther. Nucl. Med. 90: 1068, 1963

[60] Häfeli, U. O., Int. J. Pharm. 277: 19, 2004.

[61] D.D. Stark, W.G. Bradley Jr., *Magnetic Resonance Imaging* (Mosby, St. Louis, 1999)

[62] Kubaska S, Sahani D V, Saini S, Hahn P F and Halpern E 2001 Dual contrast enhanced magnetic resonance imaging of the liver with superparamagnetic iron oxide followed by

gadolinium for lesion detection and characterization *Clin. Radiol.* 56 410–5

[63] Low R N 2001 MR imaging of the liver using gadolinium chelatesMagn. Reson. Imag. Clin. N. Am. 9 717–43

[64] Gonzales, M et al (2005). Synthesis of magnetoliposomes with monodispersed iron oxides nanocrystal cores for hyperthermia. Journal of Magnetism and Magnetic Materials 293(1): 265-270

[65] Neuberger, T. et al, Journal magntism and magnetic materials (2005) 293: pp 483-496

[66] Jordan, A., et al, Journal magntism and magnetic materials (1999) 201:pp 413-419

[67] Freeman, M.N, et al, Journal of Applied Physics (1960) 31, 732

[68] S Douang, C. Tang, H. Zhao (2004), Photochemical Synthesis of Gold Nanoparticles by the Sunlight Radiation Using A Seeding Appraoch.

[69]] **(**a) Hyeon, T., Lee, S. S., Park, J., Chung, Y., Na, H. B. J Am. Chem Soc. 2001, 123, 12798. (b) Hyeon, T. Chem. Commun. 2003, 919.

[70] Teja, Amyn S.; Koh, Pei-Yoong (2009) "Synthesis, properties, and applications of magnetic iron oxide nanoparticles" progress in crystal Growth and characterization of Materials 55:22.doi

[71] R.M Cornell, U. Schwertmann. The iron-oxide: structure, properties, reactions, occurrence and uses. VCH New York, USA 1996 pp. 28-29.

[72]*Magnetospirillummagneticum*:http://www.ncbi.nlm.nih.gov/Taxonomy/taxonomyhome.html/

[73] Frankel and Bazylinski, "Magnetosome Mysteries-Despite Reasonable Progress Elucidating Magnetotactic Microorganisms, Many Questions Remain," *ASM News,* 2004, Volume 70, Number 4, p.176-183.

[74] Arakaki,A., Nakazawa,H., Nemoto,M., Mori,T. & Matsunaga,T. (2008). "Formation of magnetite by bacteria and its application". Journal of the Royal Society Interface,5, 977-999

[75] Lazaro FJ, Abadia AR, Romero MS, Gutierrez L, Lazaro J, Morales MP Biochim Biophys Acta. 2005, 1740:434–45

[76] T.K. Indira, P.K. Lakshmi. Magnetic Nanoparticles – A Review, International Journal of Pharmaceutical Sciences and Nanotechnology. 2010, Volume 3 • Issue 3

[77] J. Meng J. Fana, G. Galiana , R.T. Branca , P.L. Clasen , S. Ma , J. Zhou , C. Leuschner , C.S.S.R. Kumar ,J. Hormes , T. Otiti , A.C. Beye , M.P. Harmer , C.J. Kiely , W. Warren , M.P. Haataja a, W.O. Soboyejo "LHRH-functionalized superparamagnetic iron oxide nanoparticles for breast cancer targeting and contrast enhancement in MRI" Materials Science and Engineering C 29 (2009) 1467–1479.

[78] R. Lawaczeck, H. Bauer, T. Frenzel, M. Hasegawa, Y. Ito, K. Kito, N. Miwa, H.Tsutsui, H. Vogler, H.J. Weinmann, Acta Radiol. 38 (1977) 584–597.

[79] S.C.A. Michel, T.M. Keller, J.M. Frohlich, D. Fink, R. Caduff, B. Seifert, B. Marincek, R.A. Kubik-Huch, Radiology 225 (2002) 527–536.

[80] R.C. Semelka, T.K.G. Helmberger, Radiology 218 (2001) 27–38.

[81] W.S. Enochs, G. Harsh, F. Hochberg, R.Weissleder, J. Magn. Reson. Imaging 9 (1999) 228–232

[82] M. Shinkai, M.Yanase, M. Suzuki, et al. Intracellular hyperthermia for cancer using magnetite cationic liposomes. Journal of Magnetism and Magnetic Materials. 1999, 194, 176184.

[83] Nielsen,O.S., Horsman,M. & Overgaard,J. (2001). A future for hyperthermia in cancer treatment? European Journal of Cancer,37, 1587-1589.

[84] Babincova,M., Leszczynska,D., Sourivong,P. & Babinec,P. (2000). Selective treatment of neoplastic cells using ferritin-mediated electromagnetic hyperthermia. Medical Hypotheses,54, 177-179.

[85] Rosensweig, R.E. (2002). Heating magnetic fluid with alternating magnetic field. Journal of Magnetism and Magnetic Materials,252, 370–374.

[86] Pamplin, B. R., *Crystal Growth,* New York: Pergamon Press, 1975.

[87] Jiang, Y., "Forced Hydrolysis and Chemical Co-Precipitation," in *Handbook of Nanophase and Nanostructured Materials*, Z. L.Wang, Y. Liu, and Z. Zhang, (eds.), New York: Kluwer Academic, 2003, p. 59.

[88] Burda, C., et al., "Chemistry and Properties of Nanocrystals of Different Shapes," *Chem. Rev.*, Vol. 105, 2005, p. 1025.

[89] Alivisatos, A. P., "Naturally Aliened Nanoparticles," *Science,* Vol. 289, 2000, p. 736.

[90] J. Liu, S. Z.Qiao, Q. H. Hu,*et al*. Magnetic Nanocomposites with Mesoporous Structures: Synthesis and Applications. Small. 2011, 7, 425-443.

[91] N. A. Luechinger, R. N. Grass, E. K. Athanassiou, *et al*. Bottom-up fabrication of metal/metal nanocomposites from nanoparticles of immiscible metals. Chemistry of Materials. 2007, 22,155-160.

[92] D. K. Tiwari, J. Behari, P. Sen. Time and dose-dependent antimicrobial potential of Ag nanoparticles synthesized by top-down approach. Current Science. 2008, 95, 647-655.

[93] P. Mohanpuria, N. K. Rana, S. K.Yadav. Biosynthesis of nanoparticles: technological concepts and future applications. Journal of Nanoparticle Research. 2008, 10, 507-517.

[94] J. Zhou, C. Leuschner, C. Kumar, J.F. Hormes and W.O. Soboyejo // *Biomaterials* **27** (2006) 2001.

[95] J. Zhou, C. Leuschner, C. Kumar, J. Hormes and W.O. Soboyejo // *Materials Science and Engineering: C* **26** (2006) 1451.

CHAPTER THREE

3.0 MATERIALS AND EXPERIMENTAL METHODS

3.1 Introduction

In this section, a general overview of the experimental process was described, beginning from how the bacteria were obtained and how they were used to synthesize the magnetic nanoparticles. The characterization techniques and adhesion measurement methods are also described.

3.2 Experimental Procedure

This gives a general detail of how the magnetic nanoparticles are formed in the presence of the magnetotactic bacteria and their characterization.

3.2.1 Biosynthesis of Magnetic Nanoparticles

Since this work is based on a novel approach, fundamental and standardized steps were used to isolate, culture and synthesized the nanoparticles in the presence of magnetotactic bacteria. These will be described here in the following sub-section: materials and equipment; collection of the sample; isolation of the bacteria; preparation of media and culturing and synthesis of the magnetic nanoparticles.

3.2.2 Equipment and Materials

The following are the equipment and the materials include: a laminar flow hood, (Biosafety Cabinet Model 36204/36205 TYPE AZ), an incubator, a shaker incubator (Innova 44 Incubator series), PH meter, beakers, micropipette tips (sterile), Bijou bottles, spatula, conical flasks, sterile micropipettes, distilled water, Bunsen burners, an autoclave, L shaped spreader, Petri dishes, normal sterile water, 70% ethanol, soil sample, optical and transmission microscopes, glass slides, *Magnetospirillum magneticum*, nutrient agar and magnetic spirillum growth (MSG) medium, UV- Spectrophotometer and X-ray diffractometer.

3.2.3 Isolation of Bacteria

Two samples labeled A and B were considered in this work. Sample A, a positive control, of the *Magnetospirillum magneticum* strain AMB-1, was obtained from Princeton. Sample B, an unidentified indigenous magnetotactic bacteria, was obtained from the soil in Sheda, FCT, Nigeria. 0.5 kg of the soil sample was collected using a plastic spatula into a new polyethylene container, this was then sealed and transferred to the Sheda Science laboratory.

Serial dilution was used to reduce the colonies that would appear in each plate for easy culturing and quantification. Sample B was placed in a disinfected bijou bottle that was autoclaved for 20 minutes, Distilled water was then added to the soil sample until the amount of solute was about 1 liter. The soil sample was then stored under ambient conditions. The magnetotactic bacteria from the sample B were collected using a convectional magnetic collection methods [1].

This method uses the magnetic response of magnetotactic bacteria to magnetic fields. First, the sample was subjected to a strong magnetic field by a permanent magnet, as shown in Figure 3.1.

Figure 3.1: Sample B set up for magnetic collection method

After 5 to 6 hours the, 1 ml of the sample near the magnetic axis was collected with a sterile pipette. This was then transferred into a sterile test tube for further isolation. It is expected that the magnetotactic bacteria, which are magnetotaxis and motile in nature, will migrate towards the pole of the magnet.

A single colony of magnetotactic bacteria was produced by the Capillary Racetrack Method (CRTM) [2]. In this case, a capillary tube closed at one end with the aid of a gas flame was filled with a chemically defined medium (enriched medium), as reported by Flies et al [1]. This was achieved by the use of hypodermic syringe that was fitted to the smallest end of a Pasteur pipette. Also, at the other large end, acts as a reservoir, wetted cotton was placed.

A permanent magnet with high susceptibility was placed at the smallest tip of the arrangement for 3 hours. Since the magnetotactic bacteria are motile and move under the influence of a magnetic field, they tend to migrate towards the tip across the cotton plug in the set up. A sterile

syringe was used to collect the magnetotactic bacteria at this point for culturing in MSG medium at a buffer of pH 4, 6, 6.5, 7, 7.5, 8.5, 9, 9.5 and 12 and agar-agar MSG semi-solid medium of pH 6.7 distilled water.

3.2.4 Preparation of MSG Semi Solid Medium and Isolation of Magnetotactic Bacteria

A similar approach and compositions as in the preparation of the MSG broth medium, is adopted here. Though in this case, an agar-agar constituent was added to the MSGM solution to have a semi-solid MSG medium. This medium was inoculated and then subjected to magnetic field as shown in Figures 3.2 and 3.3.

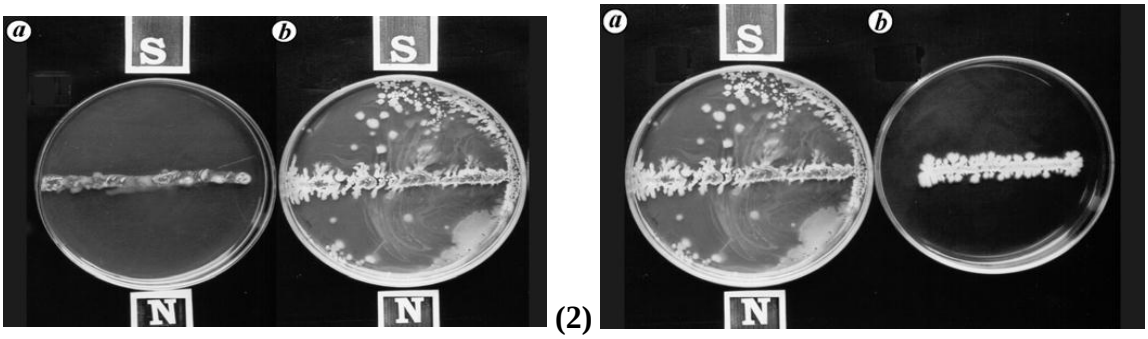

Figure 3.2: (1) (a) Response of non-MTB (b) Response of MTB to the magnetic field. (2) Response of MTB to (a) Magnetic field (b) non-magnetic field.(Magnetotactic Bacteria from Lunar lake by Mahesh S. Chavadar* and Shyam S. Bajekal)

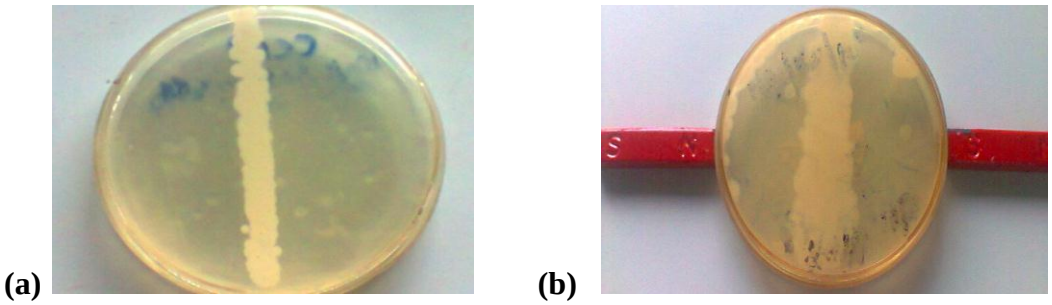

Figure 3.3: (a) Suspected MTB when not subjected (b) Suspected MTB when subjected to to a magnetic field.

This was an alternative secondary method in the purification of the indigenous magnetotactic bacteria for inoculation and synthesis in the MSG medium.

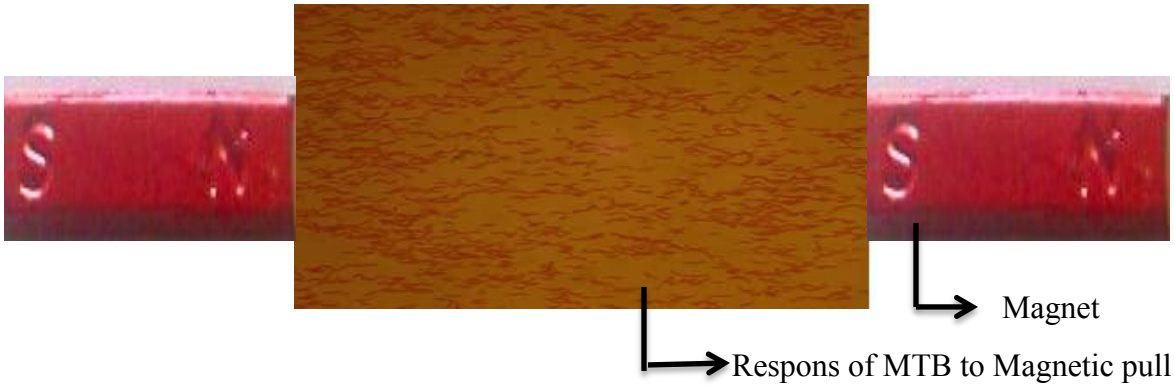

Figure 3.4: Microscopic view of MTB showing their response to magnetic pull from a field

3.2.5 Preparation of Buffer for the MSG Medium

After the purification of the magnetotactic bacteria, an acetate and phosphate buffer of pH 4, 6, 6.5, 7, 7.5, 8.5, 9, 9.5 and 12 was prepared. The acetate buffer that was used had a composition of 0.1M acetic acid and 0.1M sodium acetate (tri-hydrate) (13.6g/l), while the phosphate buffer contained 0.1M disodium hydrogen phosphate (14.2g/l), 0.1M HCl and 0.1M NaOH. These buffers were used to prepare the MSG medium for inoculation.

Figure 3.5: pH meter used during preparation of standard Buffer

3.2.6 Preparation of MSGM broth medium for inoculation and culturing of the Magnetotactic bacteria

Here, 5 ml sample A and sample B obtained from the capillary racetrack method were inoculated into the MSG broth medium under a laminar flow hood (Biosafety Cabinet Model 36204/36205 TYPE AZ) in an aseptic conditions to avoid contamination. Thereafter, the samples were place in a shaker incubator (New Brunswick Innova 44 Incubator Series Programmable, console Incubator Shaker) rotating at 141 rpm at 29^{o}C for uniformity of growth. Each of the samples was inoculated in MSG broth medium with standard buffer of pH 4, 6, 6.5, 7, 7.5, 8.5, 9, 9.5 and 12.

Figure 3.6: Prepared MSG media for inoculation in the Laminar flow hood (Biosafety Cabinet Model 36204/36205 TYPE AZ)

The MSGM medium used has a composition of 0.074 g of succinic acid, 0.068 g of KH_2PO_4, 0.012 g of sodium nitrate, 0.02% of polypeptone, 0.01% of yeast extract, 0.005% of L-cysteine, 150µg/ml of Chloramphenicol, 1 ml of Wolfe's vitamin, 0.5 ml of Wolfe's mineral and 0.2 ml (0.018g) of ferric quinate. After 24 hour the first samples were taken in an aseptic condition for bacteria and magnetite quantification.

3.2.7 Preparation of Standard Curve of Magnetite Nanoparticles from a Known Concentration

To obtain the concentration of the magnetite synthesized biologically, a standardized curve of magnetite concentration was obtained from chemically synthesized magnetite. This was used to quantify the amount (concentration) of the nanoparticles produced. A commercially acquired magnetite for the concentration curve was used, this was obtained by chemical synthesis called Solvothermal or hydrothermal method. Here, 0.65 g of ferric chloride and 0.12 g of iron powder

were added to 20 ml hexane solution containing 6.0 g of dedecylamine and 3.5 ml of oleic acid at room temperature. The resulting mixture was transferred into a 60 ml Teflon-lined stainless autoclave. The autoclave was sealed and maintained in an electric oven at 180^{o}C for 24 hours and then cooled to room temperature naturally. The product was washed in absolute ethanol several times followed by centrifugation at 1500 rpm for 5 minutes and finally dried in a vacuum at 60^{o}C for 8 hours.

The standard curve of known magnetite concentration was portrayed with absorbance at 440 nm. The procedure for the preparation of the standard curve is briefly highlighted: 0.0025g of Fe_3O_4 was dissolved in a solution of 5 ml of absolute ethanol. Eight samples were prepared with known concentrations. The absorbances of the mixtures were then determined at a wavelength of 440 nm, using a UV spectrophotometer.

The standard curve that was used to obtain the actual concentrations was obtained by measuring the actual absorbances for known concentrations of magnetite (Fe_3O_4) in solution. The absorbances were measured using a model the Camspec M550 Double Beam Scanning UV/Vis Spectrophotometer.

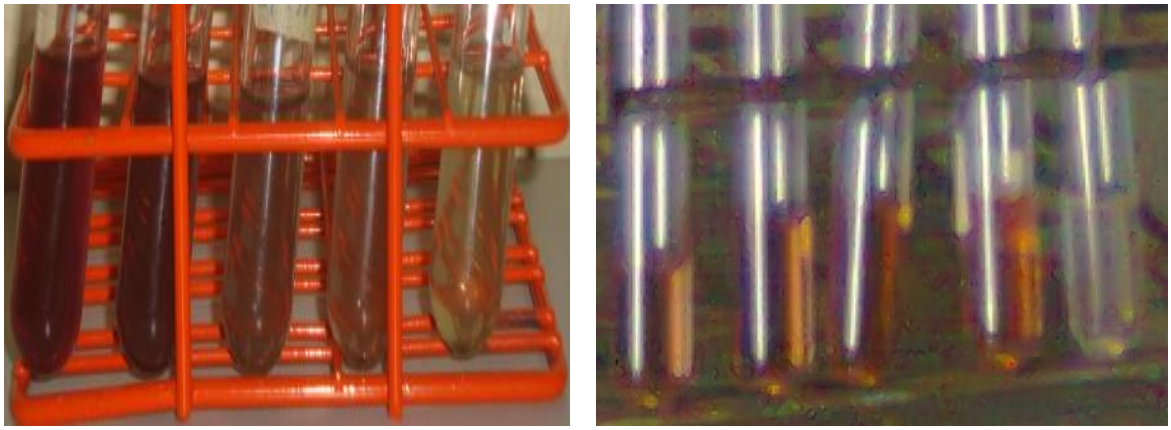

Figure 3.7: Sample of known concentrated magnetite nanoparticles prepared for standard curve

UV Visible spectroscopy is used to measures the response of a sample in the cuvette. Light

source from the lamp pass through a lens forming a monomatic light by the help of a monochromator through the sample to ultraviolet and visible range of electromagnetic radiations. The molecules and atoms of the samples have electronic transitions while most of the solids have interband transitions in the UV and Visible range. Thus, the absorbance of a solution increases as attenuation of the beam increases. The principle *Beer's Law* as described in Figure 3.7 states that absorbance is directly proportional to the path length, b, and the concentration, c, of the absorbing species is obserevd.

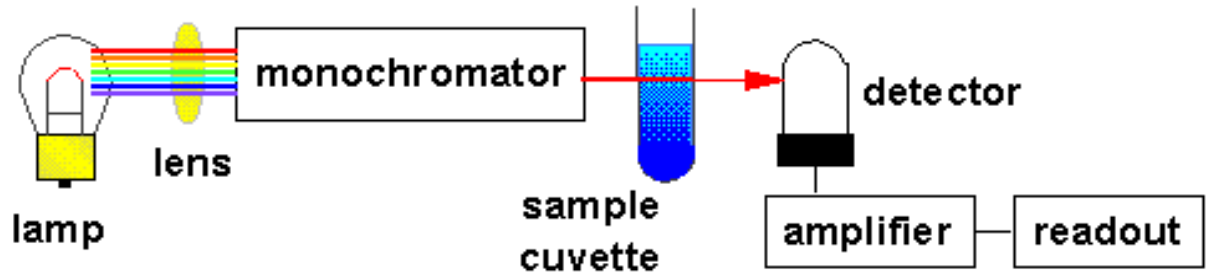

Figure 3.8: General principle of operation of the UV/Vis spectrophotometer

The results are presented in Table 3.1 in which the concentrations and measured absorbance values are summarized.

Table 3.1: Concentration and absorbance value for standard curve

Concentration in M	Absorbance (A)
0.000000	0.000
0.000108	0.190
0.000216	0.321
0.000431	0.510
0.000862	0.931
0.001293	1.400
0.001724	1.800
0.002155	2.300

3.2.8 Synthesis and quantification of the Magnetite Nanoparticles

It is expected that as the bacteria grow in the medium, the magnetite evolve intracellularly in the magnetosomes of the bacteria, as a result of synthesis, which is guided by nucleation and growth process. In some cases, the bacteria has been shown to secrete some enzymes, that are capable of synthesizing magnetic nanoparticles extracellularly. 2 ml of each sample was centrifuged at 10000 rpm for 10 minutes to separate the pellet (bacteria cell) and the supernatant. The pellet was subjected to lysis test, where the cell walls are destroyed to expose the magnetite in the magnetosomes. This was done by subjecting it to 1.0 ml of 12 M of HCl and 0.5 ml of 1.5 M of potassium thiocyanate, which turns red in color. The supernatant was also subjected to ferric chloride to reveal the magnetite content within it.

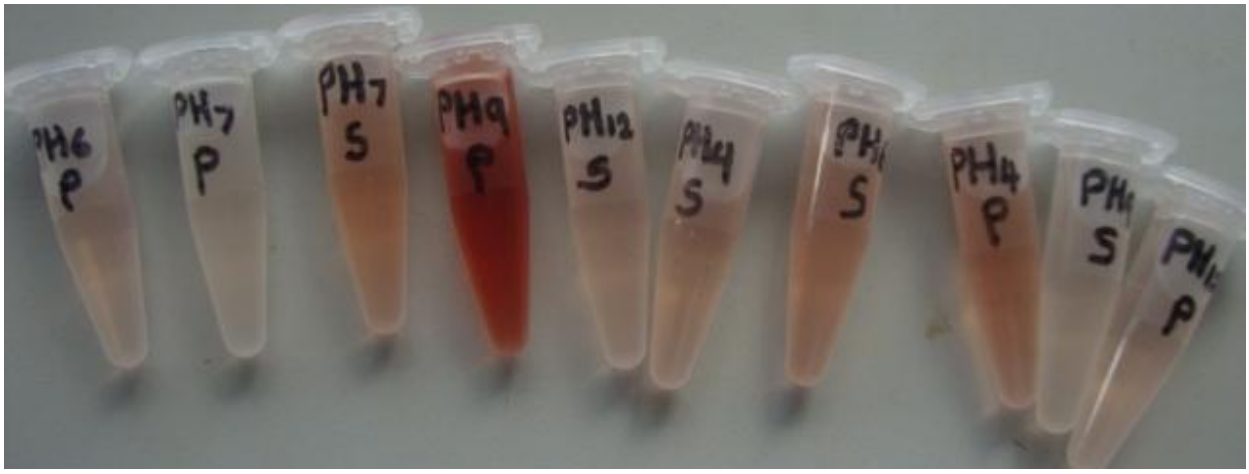

Figure 3.9: Samples of pellet and supernatant exposed to HCl and Potassium thiocyanate for Magnetite quantification and ferric chloride respectively.

This is to test intracellullarly from the pellet, and extracellularly from the supernatant, for the synthesis of magnetic nanoparticles by the bacteria. A similar spectrophotometric analysis technique (at a wavelength 440 nm) was used afterwards to determine the concentration from the

absorbance measurements. This was done using the standard curve that was produced earlier from known concentration of magnetite at a wavelength. A standard curve of known concentration from chemical synthesis of magnetite was wavelength of 440 nm. The results obtained from the absorbance measurements, obtained from the nanoparticles formed within the pellets and supernatants were recorded after 5 days of exposure to different pH conditions (4.0, 6.0, 6.5,7.0, 7.5, 8.5, 9.0, 9.5, 12.0).

3.2.9 Characterization of Nanoparticle Size and Morphology

HRTEM and LRTEM were used to view the magnetic nanoparticles formed by the samples at the different pH for five days. This is to unravel the different shapes and sizes of the magnetic nanoparticles produce with respect to the pH and time. Some of the TEM result for the two samples were analysed noting the fact that sample A represents the positive control *Magnetospirillum Magneticum,* while sample B stands for the indigenous MTB isolated.

The morphological and structural properties of the nanoparticles formed in the presence of the two different kinds of bacteria were observed by the aid of the HRTEM and LRTEM. Three pH (6.5, 7.5 and 9.5) were specifically considered for this characterization. Their respective mean size distributions and shapes were carefully analyzed and described from the TEM micrograph.

3.3 References

[1] Schuler, D. and Frankel, R. B., Bacterial magnetosomes: microbiology, biomineralization and biotechnological applications. Appl. Microbiol. Biotechnology., 1999, **52**, 464–473.

[2] Moench, T. T. and Konetzka, W. A., A novel method for the isolation and study of a magnetotactic bacterium. Arch. Microbiol., 1978, **119**, 203–212.

CHAPTER FOUR

4.0 RESULT AND DISCUSSION

4.1 Biosynthesis of magnetic nanoparticles

Two samples of magnetotactic bacteria were used in this work for the synthesis of magnetic nanoparticles. Sample A, *Magnetospirillium magneticum* from Princeton in the U.S.A and sample B, of local magnetotactic bacteria obtained from Sheda Federal Capital Territory, Abuja, Nigeria. Both types the magnetotactic bacteria synthesized magnetic nanoparticles extracellularly and intracellularly. However, the concentration of nanoparticles and the sizes and shapes of the nanoparticles varied with pH..

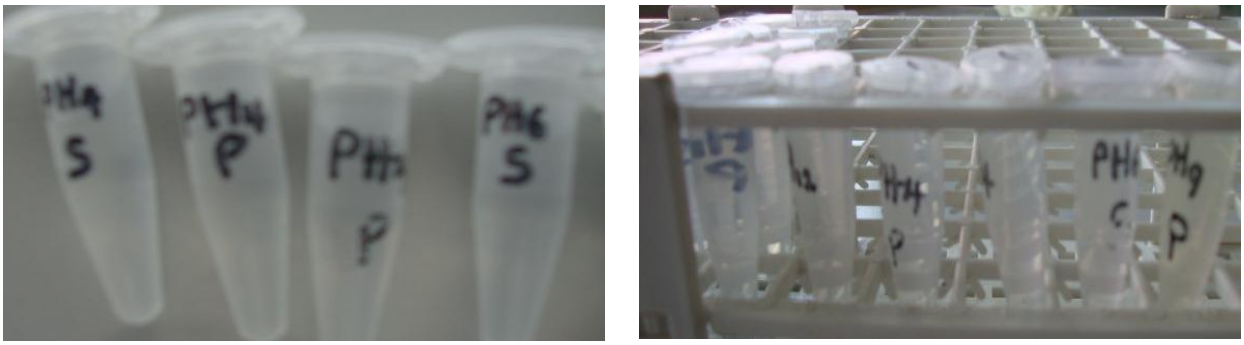

Figure 4.1: Some pellets and supernatants before chemical characterization

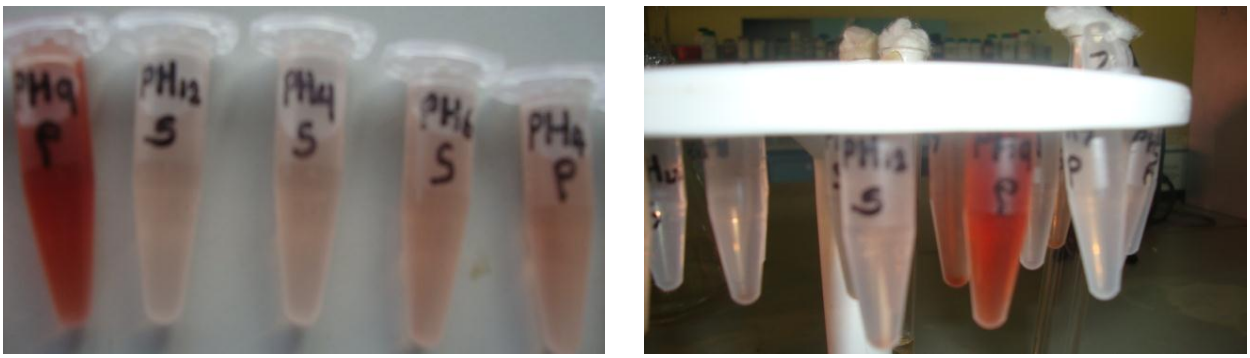

Figure 4.2: Some pellets and supernatants ready for characterization after synthesis

4.2 Characterization

Chemical characterization was carried out using a UV-spectrophotometer. This is to quantify the amount of magnetite produced. The shapes and sizes of the nanoparticles were studied using transmission electron microscopy.

4.2.1 Standard Curve

The absorbances obtained for the known concentration of chemically synthesized magnetite (Fe_3O_4) are summarized in Table 4.1. The results are also plotted in figure 4.4dependent

Table 4.1: Concentration and absorbance value for the standard curve

Concentration in M	Absorbance (A)
0.000000	0.000
0.000108	0.190
0.000216	0.321
0.000431	0.510
0.000862	0.931
0.001293	1.400
0.001724	1.800
0.002155	2.300

The absorbance of the solution with the unknown concentration was measured at the same wavelength 440nm which the standard curve was prepared. Corresponding concentration for the samples was read up from the standard curve in figure 4.3. These shows a linear dependence of concentration on absorbance, with an r^2 of 0.9962. This implies that the curve obtained obeys Beer Lambert law. The synthesized magnetite were obtained from this standard curve.

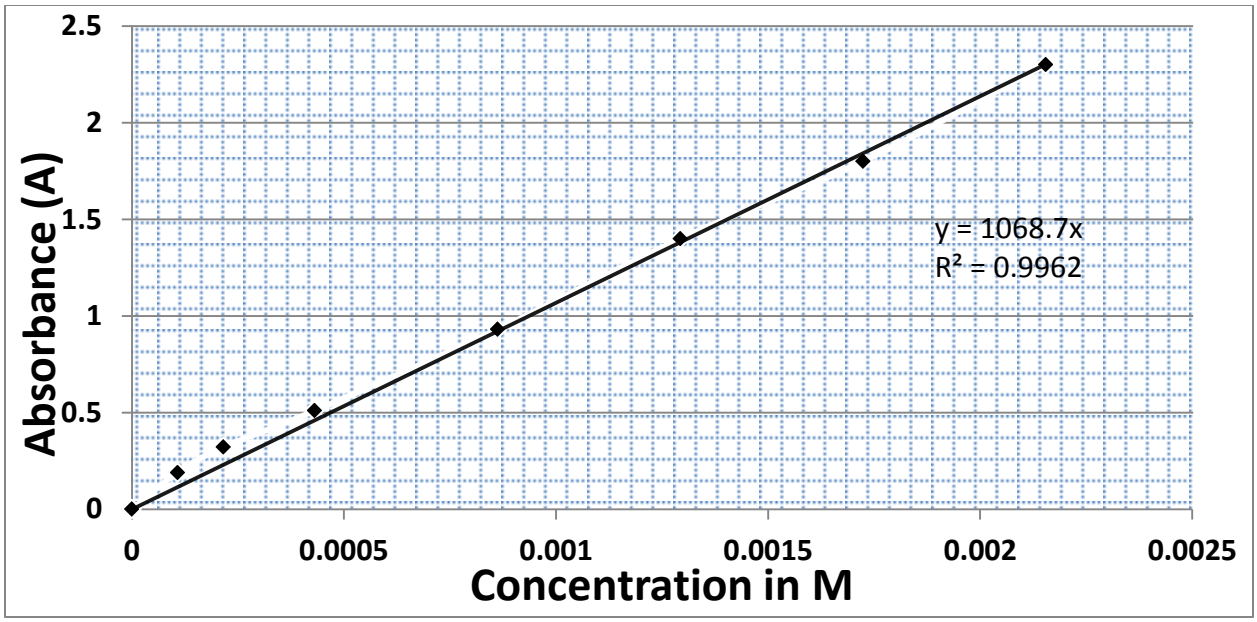

Figure 4.3: Standard curve for known concentrated magnetite nanoparticles

4.2.2 Chemical Characterization

The absorbance of the pellet and supernatant, for both the positive control and the indigenous strain samples were characterized after and completing the synthesis steps under well controlled durations and pH. This was done using a UV spectrophotometer that was operated at a wavelength of 440 nm where solution turned red in color upon absorption of light. The actual concentrations were determined from a standard curve prepared earlier shown in Figure 4.3. The results are summarized in Table 4.2 – 4.6.

Table 4.2: Absorbance data of pellet/supernatant for the samples after 24 hours (1 Days)

pH	Absorbance of Sample A (M. Magneticum)		Absorbance of sample B (Local MTB)	
	Pellet	**Supernatant**	**Pellet**	**Supernatant**
4.0	0.237	0.001	0.200	0.001
6.0	0.261	0.001	0.230	0.002
6.5	0.112	0.002	0.251	0.002
7.0	0.394	0.001	0.279	0.001
7.5	0.385	0.001	0.255	0.002
8.5	0.312	0.000	0.305	0.001
9.0	0.264	0.001	0.315	0.002
9.5	0.210	0.002	0.200	0.003
12.0	0.190	0.002	0.150	0.004

From Table 4.2 above, there is a clear indication that the absorbance of the pellets is higher than that of the suparnatants. From the experimental data obtained, it shows that, for the positive control, *Magnetospirillum Magneticum,* highest absorbance was observed at pH 7.0 and lowest absorbance at pH 6.5. In the same way, for the local strain, highest and lowest absorbance was observed at pH 9.0 and pH 12.0 respectively.

Table 4.3: Absorbance data of pellet/supernatant for the samples after 48 hours (2 Days)

pH	Absorbance of Sample A (M. Magneticum)		Absorbance of sample B (Local MTB)	
	Pellet	**Supernatant**	**Pellet**	**Supernatant**
4.0	0.254	0.001	0.210	0.002
6.0	0.271	0.002	0.246	0.003
6.5	0.194	0.002	0.276	0.002
7.0	0.433	0.000	0.299	0.002
7.5	0.422	0.002	0.286	0.001
8.5	0.367	0.002	0.349	0.001
9.0	0.286	0.001	0.362	0.003
9.5	0.222	0.002	0.210	0.004
12.0	0.219	0.003	0.180	0.005

From Table 4.3 above, there is a clear indication that the absorbance of the pellets is higher than that of the suparnatants for both samples. From the experimental data obtained, it shows that, for the positive control, *Magnetospirillum Magneticum,* highest absorbance was observed at pH 7.0 and lowest absorbance at pH 12.0. In the same way, for the local strain, highest and lowest absorbance was observed at pH 9.0 and pH 12.0 respectively.

Table 4.4: Absorbance data of pellet/supernatant for the samples after 72 hours (3 Days)

pH	Absorbance of Sample A (M. Magneticum)		Absorbance of sample B (Local MTB)	
	Pellet	**Supernatant**	**Pellet**	**Supernatant**
4.0	0.269	0.002	0.233	0.003
6.0	0.298	0.003	0.264	0.004
6.5	0.236	0.003	0.311	0.002
7.0	0.466	0.001	0.336	0.002
7.5	0.445	0.001	0.328	0.001
8.5	0.398	0.000	0.370	0.002
9.0	0.307	0.002	0.398	0.004
9.5	0.239	0.002	0.232	0.005
12.0	0.221	0.003	0.200	0.006

From Table 4.4 above, there is a clear indication that the absorbance of the pellets is higher than that of the suparnatants for both samples. From the experimental data obtained, it shows that, for the positive control, *Magnetospirillum Magneticum,* highest absorbance was observed at pH 7.0 and lowest absorbance at pH 12.0. In the same way, for the local strain, highest and lowest absorbance was observed at pH 9.0 and pH 12.0 respectively.

Table 4.5: Absorbance data of pellet/supernatant for the samples after 96 hours (4 Days)

pH	Absorbance of Sample A (M. Magneticum)		Absorbance of sample B (Local MTB)	
	Pellet	**Supernatant**	**Pellet**	**Supernatant**
4.0	0.289	0.003	0.261	0.004
6.0	0.310	0.002	0.288	0.005
6.5	0.259	0.003	0.334	0.003
7.0	0.499	0.002	0.369	0.002
7.5	0.489	0.002	0.346	0.002
8.5	0.326	0.001	0.396	0.004
9.0	0.322	0.001	0.421	0.005
9.5	0.243	0.002	0.246	0.006
12.0	0.243	0.003	0.212	0.007

From Table 4.5 above, there is a clear indication that the absorbance of the pellets is higher than that of the suparnatants for both samples. From the experimental data obtained, it shows that, for the positive control, *Magnetospirillum Magneticum,* highest absorbance was observed at pH 7.0 and lowest absorbance at pH 12.0 and 9.5. In the same way, for the local strain, highest and lowest absorbance was observed at pH 9.0 and pH 12.0 respectively.

Table 4.6: Absorbance data of pellet/supernatant for the samples after 120 hours (5 Days)

pH	Absorbance of Sample A (M. Magneticum)		Absorbance of sample B (Local MTB)	
	Pellet	**Supernatant**	**Pellet**	**Supernatant**
4.0	0.304	0.003	0.285	0.005
6.0	0.334	0.004	0.295	0.005
6.5	0.296	0.003	0.354	0.004
7.0	0.531	0.003	0.388	0.003
7.5	0.519	0.002	0.380	0.002
8.5	0.383	0.001	0.431	0.001
9.0	0.348	0.001	0.444	0.004
9.5	0.281	0.003	0.263	0.006
12.0	0.243	0.003	0.253	0.008

From Table 4.4 above, there is a clear indication that the absorbance of the pellets is higher than that of the suparnatants for both samples. From the experimental data obtained, it shows that, for the positive control, *Magnetospirillum Magneticum,* highest absorbance was observed at pH 7.0 and lowest absorbance at pH 12.0. In the same way, for the local strain, highest and lowest absorbance was observed at pH 9.0 and pH 12.0 respectively.

Again, for a given pH, the absorbance of the pellets was greater than that of the supernatant (Figures 4.2 – 4.6).

From Beer Lambert's law, this shows that the iron oxide content of the pellets was greater than that of the supernatant. Note that Beer lambert's law states that the amount of light absorbed at a specific wavelength (in this case 440 nm) is directly proportional to the concentration of the solution. Hence, the absorbance of the samples is proportional to their concentration.

The absorbance is given by:

$$\mathbf{A = \beta C \mathit{l}}$$

Where, A is the absorbance (no units), β is the molar absorptivity coefficient (L/mol-cm), C is the concentration of absorbing species (mol/L) and *l* is the path length (cm).

4.2.3 Quantification of the magnetite synthesized by MTB using Spectrophotometric Ananlysis

The pH and time dependent of magnetite formation was determine from the absorbance measurement and the standard curve (Figure 4.3). The results are presented in table 4.7 – 4.10 and Figure 4.4 – 4.7, for magnetite synthesis from *Magnetospirillu Magneticum*and and the local

strain respectively. The measured concentrations are clearly dependent on pH, with the highest concentrations occurring at pH of ~ 7.0 and 9.0 for the *Magnetospirillu Magneticum* and the local strain respectively.

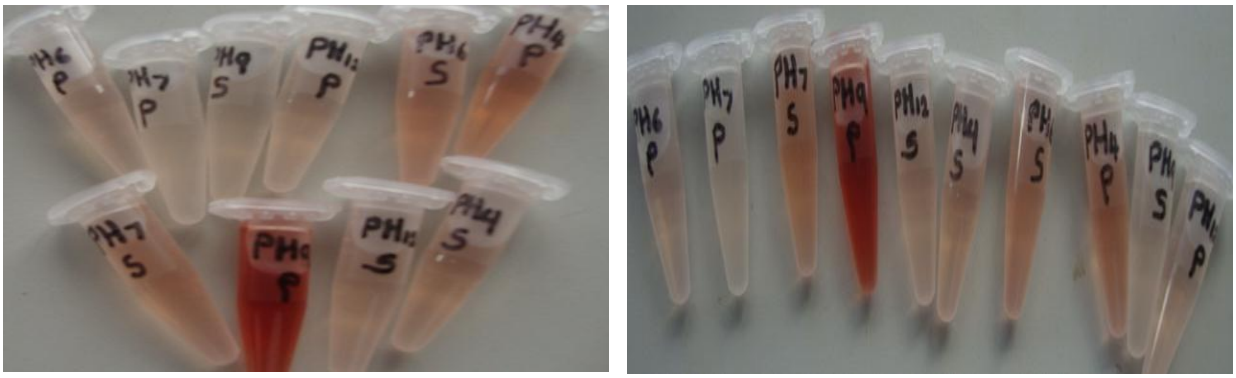

Figure 4.4: Some pellets and supernatant of the samples after complete synthesis

The table below shows the concentration data for Sample A pellet for five days.

Table 4.7: Concentration data for M. *magneticum (S*ample A) pellet for five days at different pH

pH	**Concentration in M of magnetite from sample A (M. *Magneticum*) Pellet**				
	Day 1	**Day 2**	**Day 3**	**Day 4**	**Day 5**
4.0	0.000222	0.000238	0.000252	0.000270	0.000284
6.0	0.000244	0.000254	0.000279	0.000290	0.000313
6.5	0.000105	0.000182	0.000221	0.000242	0.000277
7.0	0.000368	0.000405	0.000436	0.000467	0.000497
7.5	0.000360	0.000395	0.000416	0.000455	0.000485
8.5	0.000291	0.000343	0.000372	0.000305	0.000358
9.0	0.000247	0.000268	0.000287	0.000301	0.000326
9.5	0.000197	0.000208	0.000224	0.000227	0.000263
12.0	0.000178	0.000205	0.000207	0.000215	0.000227

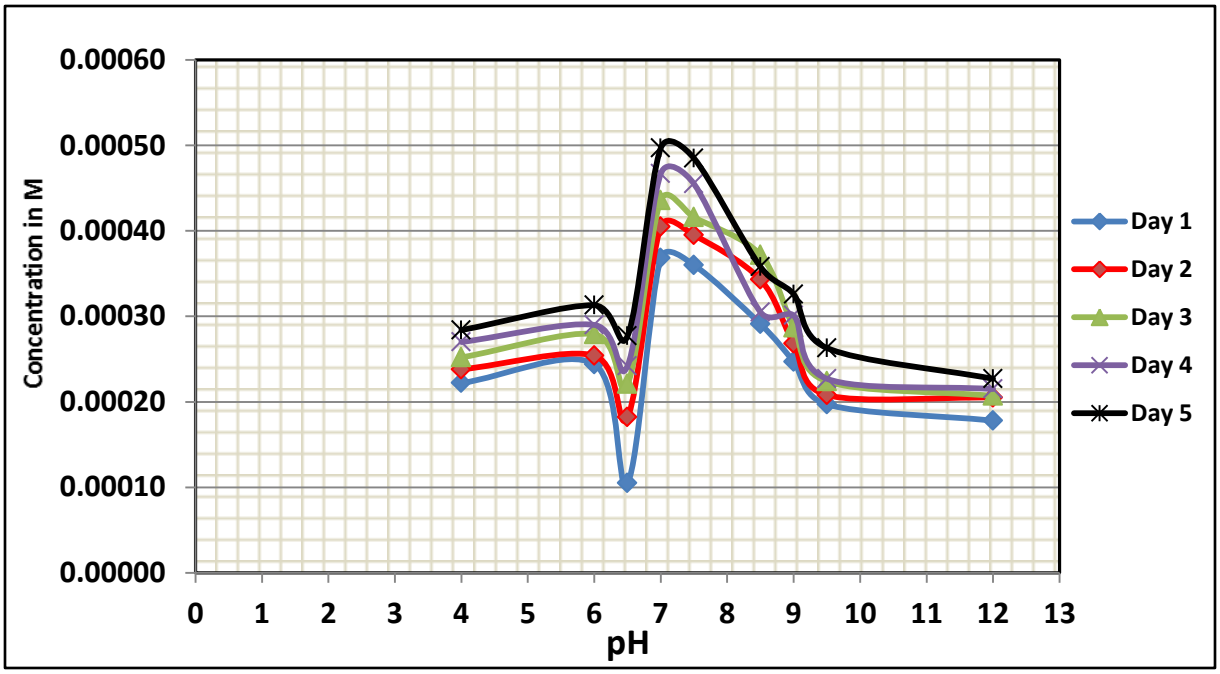

Figure 4.5: Concentration-pH curve for the M. *magneticum* pellet at different days

However, the results suggest that the optimal conditions for the synthesis of the magnetite from the *Magnetospirillum Magneticum* pellets corresponds to the neutral pH 7. In contrast, the least favourable pH values for the formation of magnetite corresponds to a pH of ~ 6.5 or 12. Similar trends were observe over the range of pH values. However, the concentration of magnetite depended on the time of exposure of the ferric chloride to *Magnetospirillum Magneticum.*

Table 4.8: Concentration data for the local strain (Sample B) pellet for five days at different pH

pH	Concentration in M of magnetite from sample B (Local MTB) Pellet				
	Day 1	**Day 2**	**Day 3**	**Day 4**	**Day 5**
4.0	0.000187	0.000197	0.000218	0.000244	0.000267
6.0	0.000215	0.000230	0.000247	0.000269	0.000295
6.5	0.000235	0.000258	0.000291	0.000313	0.000354
7.0	0.000261	0.000300	0.000314	0.000345	0.000388
7.5	0.000239	0.000268	0.000307	0.000324	0.000380
8.5	0.000285	0.000327	0.000346	0.000371	0.000431
9.0	0.000295	0.000339	0.000372	0.000394	0.000444
9.5	0.000187	0.000197	0.000217	0.000230	0.000263
12.0	0.000140	0.000168	0.000187	0.000198	0.000253

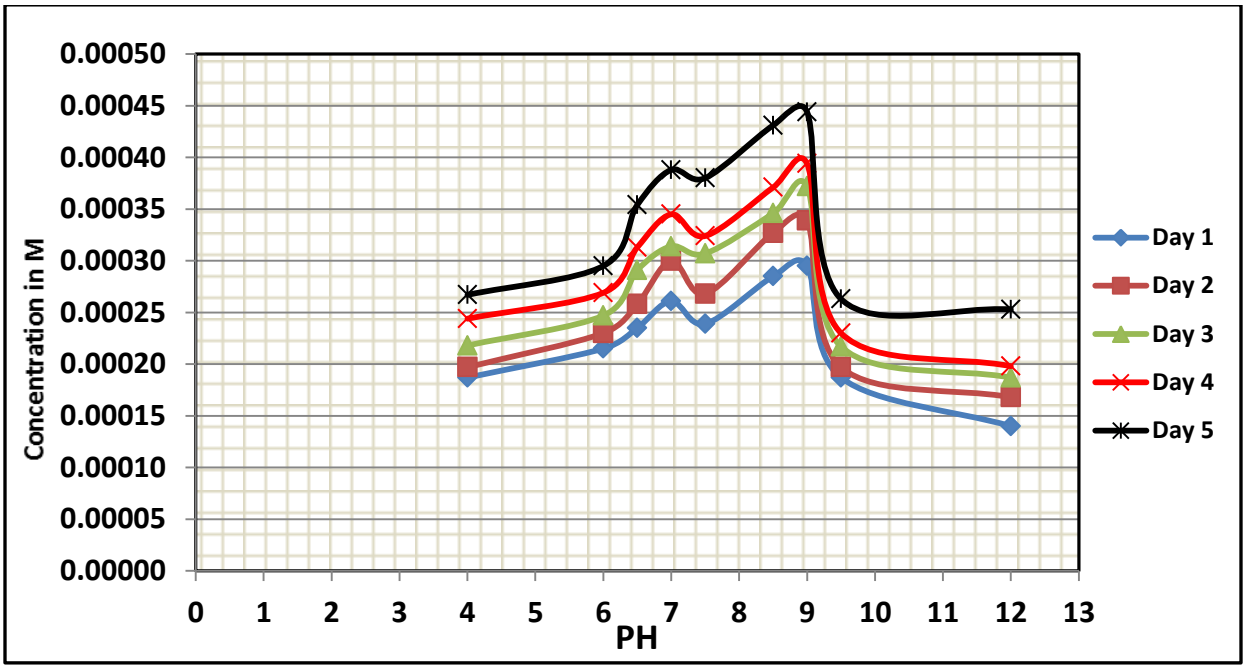

Figure 4.6: Concentration-pH curve for the local strain pellet at different days

The result obtained from the local strain (sample B) are presented in Table 4.8 and Figure 4.6. these result shows that, the highest concentration of magnetite corresponds to a pH of ~ 8.5, while the lowest concentrations are obtained for high pH values between ~ 9 and 12. Reasons for the above trends are not fully understood at the moment.

Table 4.9: Concentration data for M. magneticum (Sample A) Supernatant for five days at different pH

PH	Concentration in M of magnetite from sample A (M. Magneticum) Supernatant				
	Day 1 x 10^{-6}	**Day 2 x 10^{-6}**	**Day 3 x 10^{-6}**	**Day 4 x 10^{-6}**	**Day 5 x 10^{-6}**
4.0	0.94	0.94	1.87	2.81	2.81
6.0	0.94	1.87	2.81	1.87	3.74
6.5	1.87	1.87	2.81	2.81	2.81
7.0	0.94	0.00	0.94	1.87	2.81
7.5	0.94	1.87	0.94	1.87	1.87
8.5	0.00	1.87	0.00	0.94	0.94
9.0	0.94	0.94	1.87	0.94	1.87
9.5	1.87	1.87	1.87	1.87	2.81
12.0	1.87	2.81	2.81	2.87	2.81

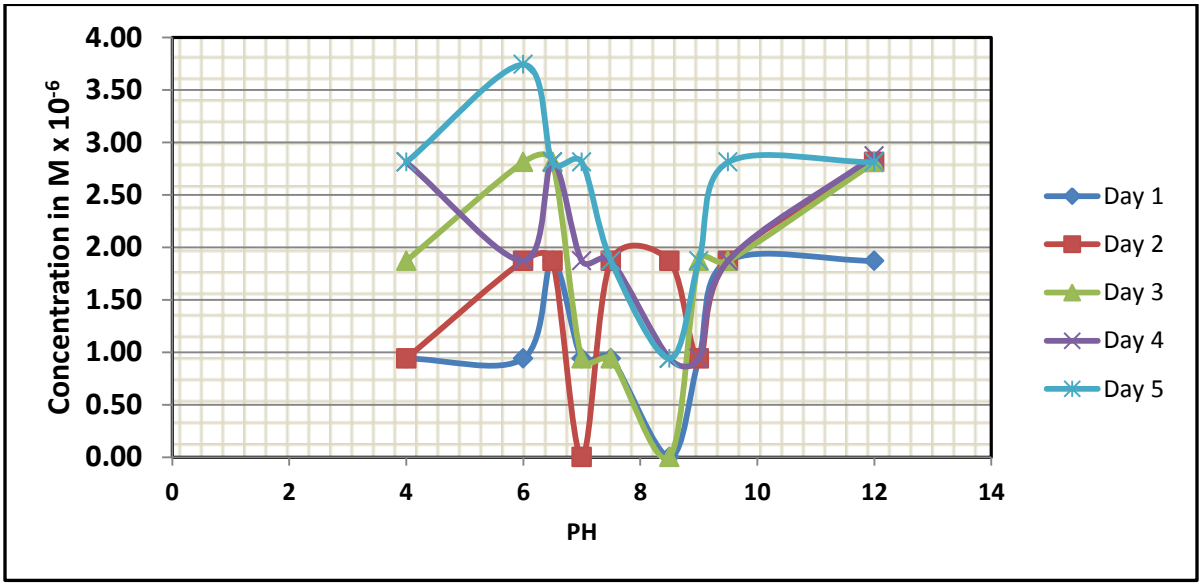

Figure 4.7: Concentration-pH curve for the M. *magneticum* supernatant at different days

The results obtained for the synthesis of magnetite from the supernatant of *Magnetospirillum Magneticum* are presented in Table 4.9 and Figure 4.7. No clear trend is obvious in the data. However, the concentration of magnetite produced from the supernatants of *Magnetospirillum Magneticum* (Figure 4.7) iwas much less than that produced from *Magnetospirillum Magneticum* pellets (Table 4.7 and Figure 4.5) at same pH values and duration of exposure of ferric chloride.

Table 4.10: Concentration data for sample A (the indigenous strain) supernatant for five days at different pH

PH	Concentration in M of magnetite from sample B (Local MTB) Supernatant				
	Day 1 x 10^{-6}	Day 2 x 10^{-6}	Day 3 x 10^{-6}	Day 4 x 10^{-6}	Day 5 x 10^{-6}
4.0	0.94	1.87	2.81	3.74	4.68
6.0	1.87	2.81	3.74	4.68	4.68
6.5	1.87	1.87	1.87	2.81	3.74
7.0	0.94	1.87	1.87	1.87	2.81
7.5	1.87	0.94	0.94	1.87	1.87
8.5	0.94	0.94	1.87	3.74	0.94
9.0	1.87	2.81	3.74	4.68	3.74
9.5	2.81	3.74	4.68	5.61	5.61
12.0	3.74	4.68	5.61	6.55	7.49

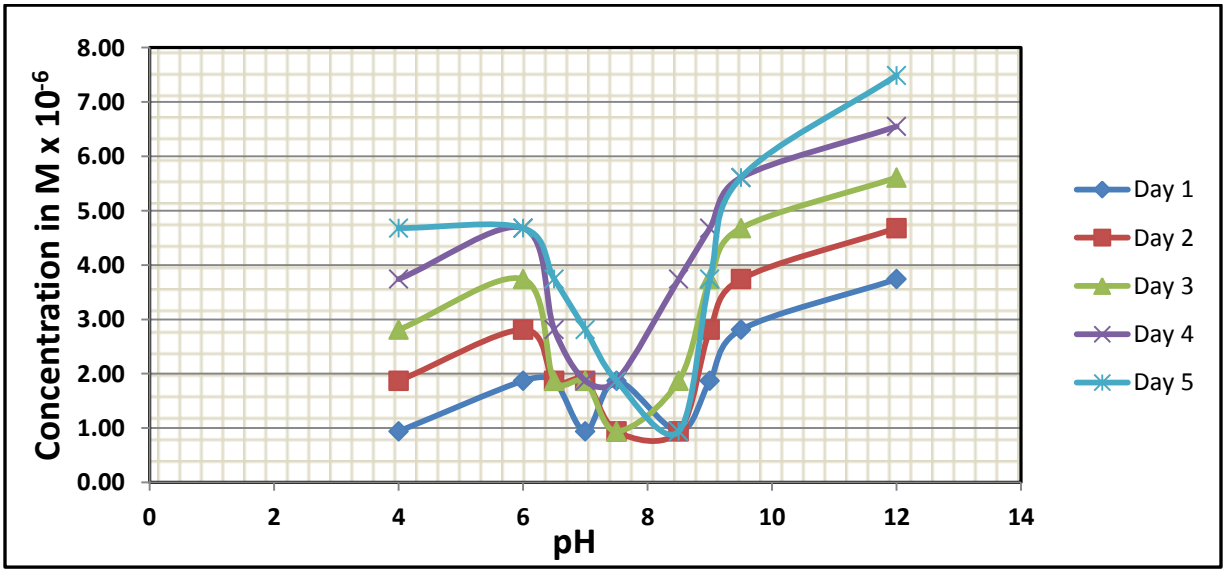

Figure 4.8: Concentration-pH curve for the supernatant of local MTB at different days

Finally, the concentration of magnetite produced from the exposure of ferric chloride to the supernatant of the local strain of bacteria are presented in Table 4.10 an Figure 4.8. The trends in the plots vary with the duration of exposure. However, the reasons for the pots are not well understood at the momen. Nevertheless, it is to note that the highest concentrations of magnetite were obtained for a pH of ~ 12 after 5 days of exposure to ferric chloride. The minimum concentrations of magnetite were obtained for pH alues of 8.5 for duration of exposure between 1 and 5 days.

4.3 TEM Results

The results of the transmission electron microscopy (TEM) analysis of the particle sizes and shapes are presented in TEM micrographs below for the magnetite synthesized directly from *Magnetospirillum Magneticum* and the yet to be identified magnetotactic local strain at a pH of ~ 6.5, 7.5 and 9.5. These results shows that the mean sizes obtained for the different duration of exposure of ferric chloride are different which explain the fact that the shapes and sizes are pH and time dependent.

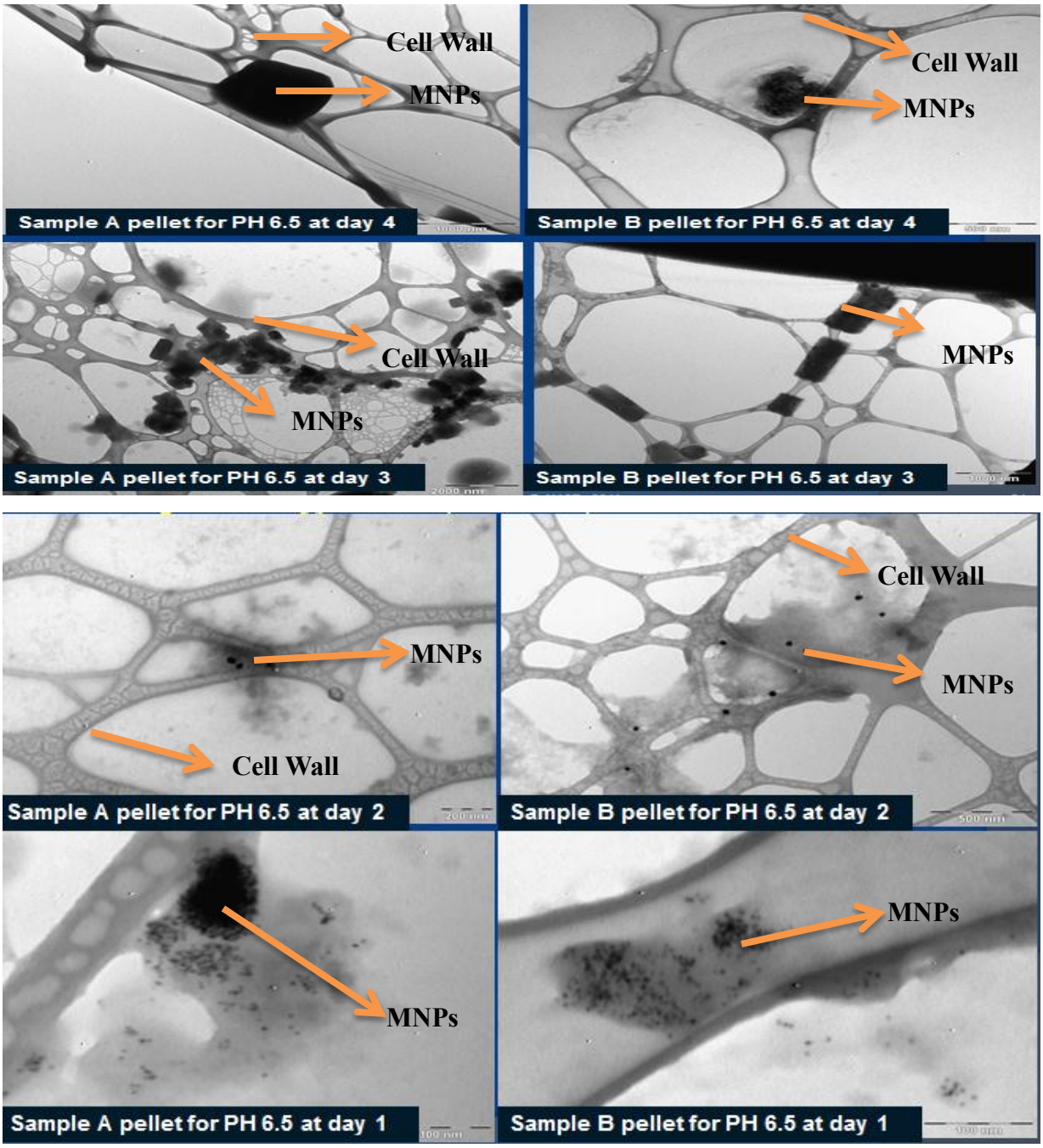

Figure 4.9: Some TEM micrograph for pH 6.5 at day 4, 3, 2 and 1 of the *Magnetospirillum Magneticum* (sample A) and Indigenous MTB (sample B) respectively.

The mean particle sizes obtained for the different durations of exposure of ferric chloride are presnted in Table 4.11 and Figure 4.10. the variations in the particle sizes, for a given duration of exposure, are also summarized in Table 4.11.

Table 4.11: The Mean particle size for pH 6.5 at different days for the Indigenous strain isolated and *Magnetospirillum Magneticum* respectively

(a)

Day	Mean particle size (nm)
Day 1	15 ± 3
Day 2	19 ± 4
Day 3	28 ± 2
Day 4	32 ± 3
Day 5	26 ± 4

(b)

Day	Mean particle size (nm)
Day 1	18 ± 2
Day 2	22 ± 3
Day 3	26 ± 4
Day 4	29 ± 3
Day 5	24 ± 4

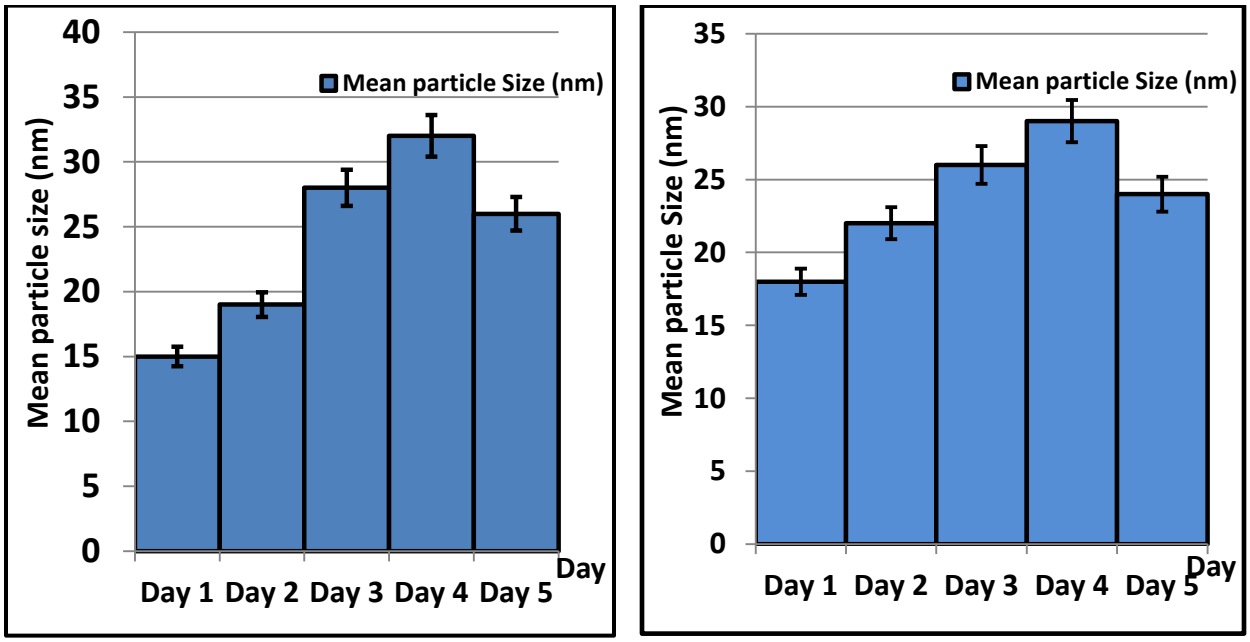

Figure 4.10: Statistical analysis showing the mean particle size distribution for pH 6.5 at different days for the Indigenous strain isolated and *Magnetospirillum magneticum* respectively.

The results from the TEM images provides useful insights into the evolution of particle shape. Following one day of exposure of *Magnetospirillum magneticum* to ferric chloride, the resulting magnetite nanoparticles were predominantly spherical (Figure 4.9). By the fourth day, the magnetite nanoparticles had pyramidal shapes (see Figure 4.9), while those formed after 5 days were essentially cuboidal in shape (see Figure 4.9). Further work is clearly needed to develop a fundamental understanding of the observed changes in nanoparticle morphology.

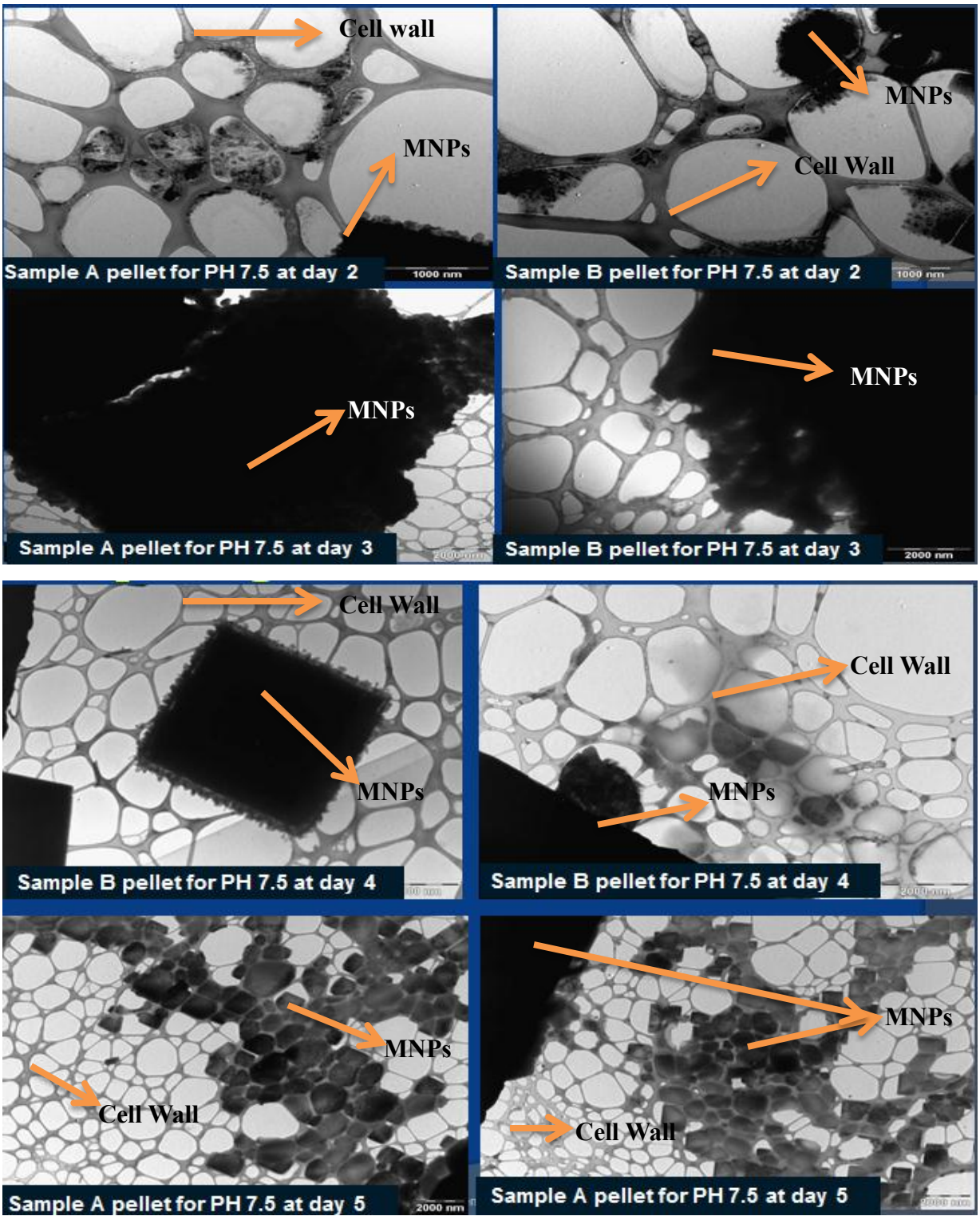

Figure 4.11: Some TEM micrograph for pH 7.5 at day 2, 3, 4 and 5 of the *Magnetospirillum Magneticum* (sample A) and Indigenous MTB (sample B) respectively

The mean particle sizes obtained for the different durations of exposure of ferric chloride are presented in Table 4.12 and Figure 4.12. the variations in the particle sizes, for a given duration of exposure, are also summarized in Table 4.12

Table 4.12: The Mean particle size for pH 7.5 at different days for the Indigenous strain isolated and *Magnetospirillum Magneticum* respectively

(a)

Day	Mean particle size (nm)
Day 1	45 ± 3
Day 2	25 ± 4
Day 3	43 ± 3
Day 4	18 ± 4
Day 5	58 ± 4

(b)

Day	Mean particle size (nm)
Day 1	38 ± 2
Day 2	41 ± 4
Day 3	28 ± 3
Day 4	21 ± 3
Day 5	52 ± 4

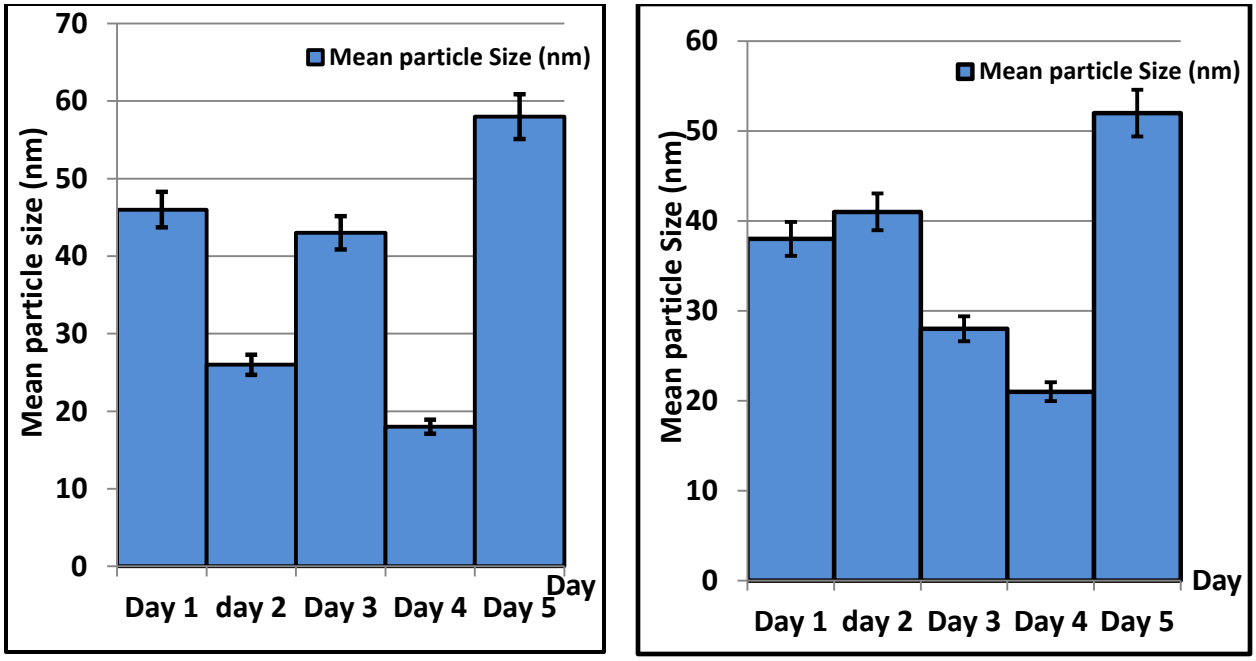

Figure 4.12: Statistical analysis showing the mean particle size distribution for pH 7.5 at different days for the Indigenous strain isolated and *Magnetospirillum magneticum* respectively.

The TEM micrograph in Figure 4.11 are the product of nanoparticles synthesis obtain for pH 7.5 using the positive control (*Magnetospirillum magneticum*) as well as the local strain. In both

case, the particle shapes evolved significantly with time. After 1 day of exposure, the nanoparticle were predominantly spherical (see Figure 4.11 above). However, by the third day, they were predominantly cuboidal in shape. By days 4 and 5, the particles shapes were essentially spherical. Finally, the sizes of the corresponding nanoparticles shown in Figure 4.12 above. Once again, the reasons for the changes in particle shape are not fully understood at the moment.

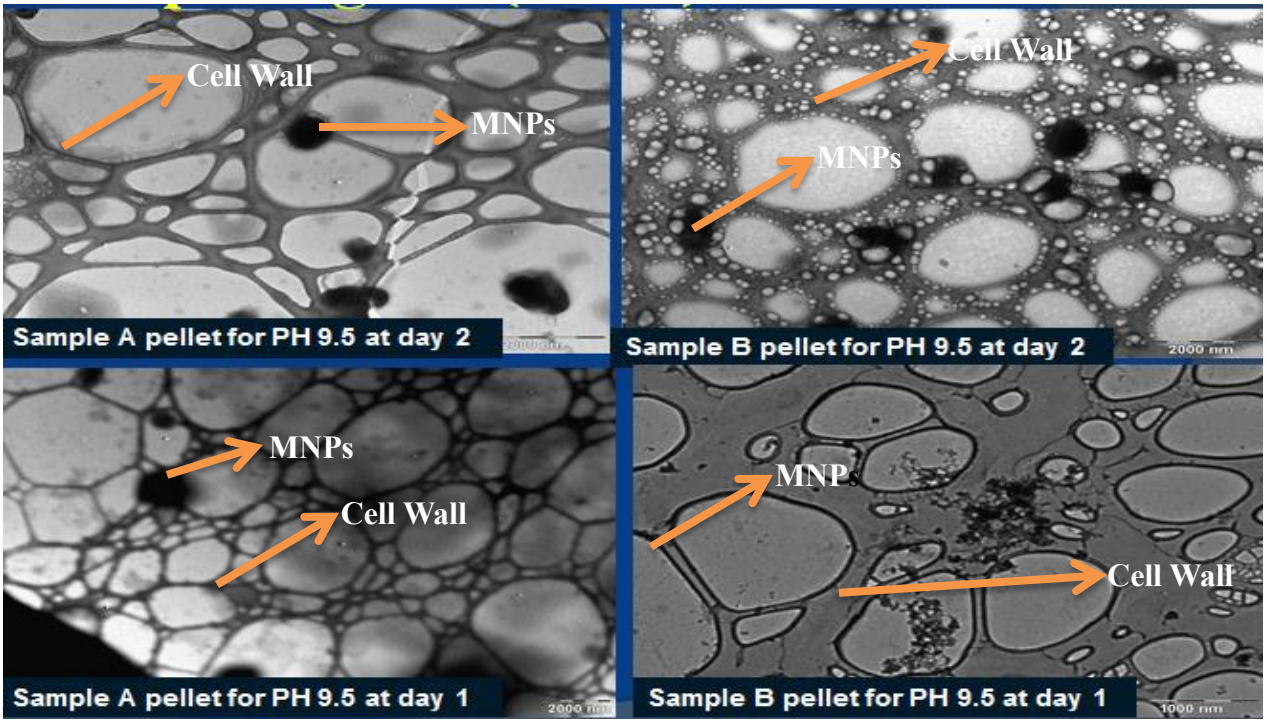

Figure 4.13: Some TEM micrograph for pH 9.5 at day 2, and 1 of the *Magnetospirillum Magneticum* (sample A) and Indigenous MTB (sample B) respectively.

The mean particle sizes obtained for the different durations of exposure of ferric chloride are presented in Table 4.13 and Figure 4.14. the variations in the particle sizes, for a given duration of exposure, are also summarized in Table 4.13.

Table 4.13: The Mean particle size for pH 9.5 at different days for the Indigenous strain isolated and *Magnetospirillum Magneticum* respectively

(a)

Day	Mean particle size (nm)
Day 1	33 ± 3
Day 2	21 ± 2
Day 3	43 ± 3
Day 4	58 ± 2
Day 5	41 ± 4

(b)

Day	Mean particle size (nm)
Day 1	33 ± 4
Day 2	21 ± 2
Day 3	43 ± 3
Day 4	58 ± 4
Day 5	41± 3

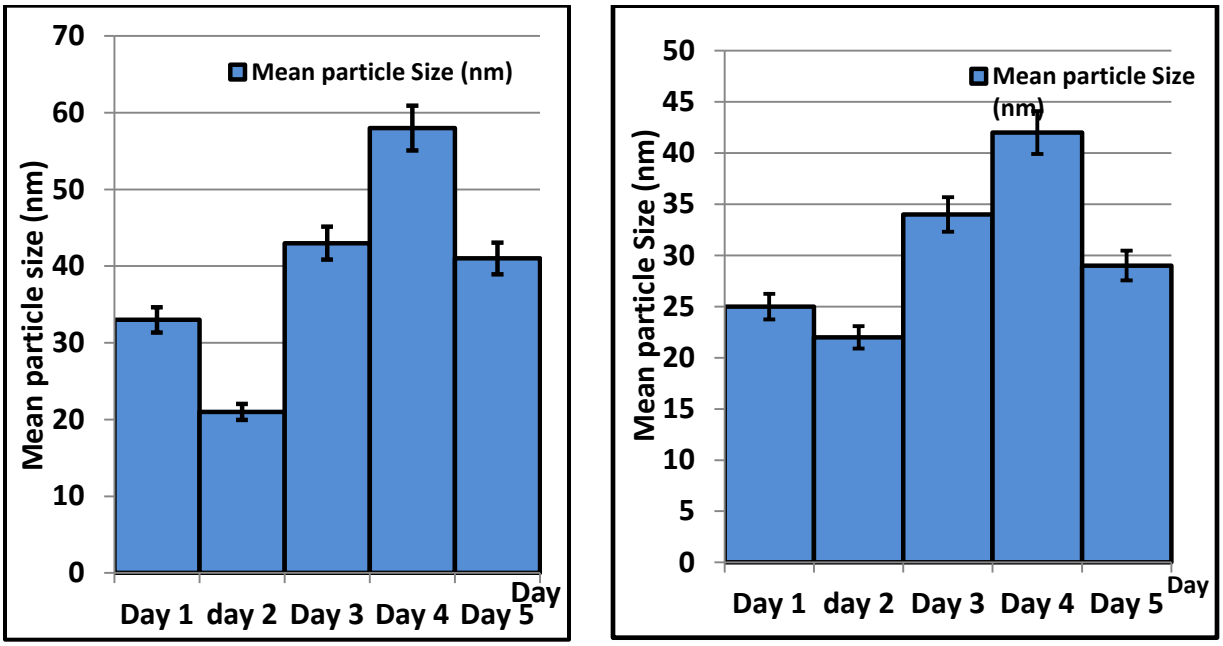

Figure 4.14: Statistical analysis showing the mean particle size distribution for pH 9.5 at different days for the Indigenous strainisolated and *Magnetospirillum magneticum* respectively.

From the TEM micrograph in figure 4.13, size and shape analysis, it was deduced for both samples that: At day 1, the particles lookspredominantly spherical. At day 2, the particles look

predominantly shapeless. At day 3, the particles look predominantly triangular. At day 4, the particles look predominantly shapeless. At day 5, the particles look predominantly rectangular.

4.4 Implications

The above results show clearly that *Magnetospirillum magneticum* and the local strain of the bacteria promote the formation of magnetite (Figure). The supernatant from *Magnetospirillum magneticum* and the local strains of bacteria also promote lower concentration of magnetite (Figure). However, further work is needed to determine the mechanisms of nanoparticle formation.

In general, the processes involved in the formation of crystalline materials from biological cells are often described as biomineralization. Such processes may include biologically induced mineralization (BIM) and biologically controlled mineralization (BCM), as suggested by Lowsenstam (1981) and Weiner (1989). In the case of BIM, nanoparticles may be formed extracellularly by reactions between metabolic by-products and the ferric chloride. However, for BCM, the nanoparticles are synthesized intracellularly by reactions between the cell constituent and the ferric chloride.

Further work is clearly needed to establish which of the above processes apply. There is also a need to understand the chemical species involved in the reduction of Fe^{3+} to Fe^{2+} as well as the nucleation and growth processes involved in the formation and growth of the crystals. These are clearly challenges for the future work. In any case, the ability to form magnetite from biosynthetic pathways may pave the way forward for the synthesis of magnetite nanoparticles for future applications in nano-medicine.

CHAPTER FIVE

5.0 SUMMARY, CONCLUSION AND RECOMMENDATION FOR FUTURE WORK

5.1 Summary and Concluding Remarks

In this work, a novel approach was used for the synthesis of magnetite nanoparticles from ferric chloride. The formation of magnetite was promoted by interaction between ferric chloride and *Magnetospirillum Magneticum* or a local strain of magnetotactic bacteria. The resulting particles had sizes that varied between ~ 15 and 60 nm after processing duration ~ 1 – 5 days. The particle shape and sizes alo demanded strongly on pH and exposure duration.

In the case of magnetite produced from *Magnetospirillum Magneticum*, the initial particle shapes for the pH of 6.5 is predominantly spherical and becomes square like predominantly by day five. In the case of magnetite produced from the local strain of bacteria, similar trend was observed at the pH and exposure time. Considering pH 7.5, the particle shapes were initially predominantly spherical, cuboidal and spherical at the end of the duration considered. Finally, for pH 9.5 discussed, the initial particles were predominantly spherical, shapeless, and rectangular and triangular in shape.

5.2 Recommendation for Future work

Further work is needed to determine the cell constituents and the reaction pathways that give rise to magnetite nanoparticles formation. The nucleation and growth mechanisms associated with biomineralization also require careful theretical, computational and experimental studies that

could guide the future scale-up of biosynthesis pathways.

Furthermore, since the cell structures and processes are informed by the genome, further work is needed to understand the effects of genomic and protomic manipulations of the cells. This could provide the basis for the future engineering of microorganisms that could increase the yield of magnetite nanoparticles produced by biosynthetic pathways.

However, much work is also needed to improve the synthesis efficiency and the control of particle size and morphology. It is thought that the synthesis of nanoparticles using microorganisms is a quite slow process (several hours and even a few days) compared to physical and chemical approaches. However, reduction of synthesis time will make this biosynthesis route much more attractive. With a better understanding of the synthesis mechanism on a cellular and molecular level, including isolation and identification of the compounds responsible for the reduction of nanoparticles, it is expected that short reaction time and high synthesis efficiency can be obtained. Thus, more research should be carried out in manipulating cells at the genomic and proteomic levels.

Effective control of the particle size and monodispersity must be thoroughly investigated. Several studies have shown that the nanoparticles formed by microorganisms may be decomposed after a certain period of time. Thus, the stability of nanoparticles produced by biological methods deserves further study and should be enhanced.

Further characterization of MNPs using AFM, MFM and XRD is necessary. Also, the adhesion

of NPs to breast cancer and normal cells, ligand-conjugations of MRI to MNPs and particles entry into cancer cells: In-vitro and in-vivo experiment should be performed using the nanoparticles from the synthesis. Modeling of nanoparticles entry into cancer cells, MRI of breast tissue in cancer cells and normal breast tissue, the effectiveness of sizes and shapes morphology in the detection and treatment of breast cancer should be the way forward to be exploited. Finally, animal trial as well as clinical trial should be carried out to ascertain the effectiveness of the biosynthetic nanoparticles in the detection and treatment of cancer with respect to other kind of synthesis.

Finally, the potential applications of magnetite to nano-medicine need to be further explored. These include the potential applications of magnetite to breast cancer/prostrate cancer detection and as well as possible application in the detection and treatment of cardiovascular disease. Potential work includes the screening of ligands for the specific detection of cancer or cardiovascular disease, or the localized treatment of such conditions by the targeted and controlled release of drugs. These are clearly some of the challenges for future work.